



**IJOER**  
RESEARCH JOURNAL

ISSN

2395-6992

# International Journal of Engineering Research & Science

[www.ijoer.com](http://www.ijoer.com)

[www.adpublications.org](http://www.adpublications.org)

Volume-9! Issue-11! November, 2023 [www.ijoer.com](http://www.ijoer.com) ! [info@ijoer.com](mailto:info@ijoer.com)

## Preface

We would like to present, with great pleasure, the inaugural volume-9, Issue-11, November 2023, of a scholarly journal, *International Journal of Engineering Research & Science*. This journal is part of the AD Publications series *in the field of Engineering, Mathematics, Physics, Chemistry and science Research Development*, and is devoted to the gamut of Engineering and Science issues, from theoretical aspects to application-dependent studies and the validation of emerging technologies.

This journal was envisioned and founded to represent the growing needs of Engineering and Science as an emerging and increasingly vital field, now widely recognized as an integral part of scientific and technical investigations. Its mission is to become a voice of the Engineering and Science community, addressing researchers and practitioners in below areas

Chemical Engineering	
Biomolecular Engineering	Materials Engineering
Molecular Engineering	Process Engineering
Corrosion Engineering	
Civil Engineering	
Environmental Engineering	Geotechnical Engineering
Structural Engineering	Mining Engineering
Transport Engineering	Water resources Engineering
Electrical Engineering	
Power System Engineering	Optical Engineering
Mechanical Engineering	
Acoustical Engineering	Manufacturing Engineering
Optomechanical Engineering	Thermal Engineering
Power plant Engineering	Energy Engineering
Sports Engineering	Vehicle Engineering
Software Engineering	
Computer-aided Engineering	Cryptographic Engineering
Teletraffic Engineering	Web Engineering
System Engineering	
Mathematics	
Arithmetic	Algebra
Number theory	Field theory and polynomials
Analysis	Combinatorics
Geometry and topology	Topology
Probability and Statistics	Computational Science
Physical Science	Operational Research
Physics	
Nuclear and particle physics	Atomic, molecular, and optical physics
Condensed matter physics	Astrophysics
Applied Physics	Modern physics
Philosophy	Core theories

Chemistry	
Analytical chemistry	Biochemistry
Inorganic chemistry	Materials chemistry
Neurochemistry	Nuclear chemistry
Organic chemistry	Physical chemistry
Other Engineering Areas	
Aerospace Engineering	Agricultural Engineering
Applied Engineering	Biomedical Engineering
Biological Engineering	Building services Engineering
Energy Engineering	Railway Engineering
Industrial Engineering	Mechatronics Engineering
Management Engineering	Military Engineering
Petroleum Engineering	Nuclear Engineering
Textile Engineering	Nano Engineering
Algorithm and Computational Complexity	Artificial Intelligence
Electronics & Communication Engineering	Image Processing
Information Retrieval	Low Power VLSI Design
Neural Networks	Plastic Engineering

Each article in this issue provides an example of a concrete industrial application or a case study of the presented methodology to amplify the impact of the contribution. We are very thankful to everybody within that community who supported the idea of creating a new Research with IJOER. We are certain that this issue will be followed by many others, reporting new developments in the Engineering and Science field. This issue would not have been possible without the great support of the Reviewer, Editorial Board members and also with our Advisory Board Members, and we would like to express our sincere thanks to all of them. We would also like to express our gratitude to the editorial staff of AD Publications, who supported us at every stage of the project. It is our hope that this fine collection of articles will be a valuable resource for *IJOER* readers and will stimulate further research into the vibrant area of Engineering and Science Research.



Mukesh Arora  
(Chief Editor)

## **Board Members**

### **Mr. Mukesh Arora (Editor-in-Chief)**

BE (Electronics & Communication), M.Tech (Digital Communication), currently serving as Assistant Professor in the Department of ECE.

### **Prof. Dr. Fabricio Moraes de Almeida**

Professor of Doctoral and Master of Regional Development and Environment - Federal University of Rondonia.

### **Dr. Parveen Sharma**

Dr Parveen Sharma is working as an Assistant Professor in the School of Mechanical Engineering at Lovely Professional University, Phagwara, Punjab.

### **Prof. S. Balamurugan**

Department of Information Technology, Kalaingar Karunanidhi Institute of Technology, Coimbatore, Tamilnadu, India.

### **Dr. Omar Abed Elkareem Abu Arqub**

Department of Mathematics, Faculty of Science, Al Balqa Applied University, Salt Campus, Salt, Jordan, He received PhD and Msc. in Applied Mathematics, The University of Jordan, Jordan.

### **Dr. AKPOJARO Jackson**

Associate Professor/HOD, Department of Mathematical and Physical Sciences, Samuel Adegboyega University, Ogwa, Edo State.

### **Dr. Ajoy Chakraborty**

Ph.D.(IIT Kharagpur) working as Professor in the department of Electronics & Electrical Communication Engineering in IIT Kharagpur since 1977.

### **Dr. Ukar W. Soelistijo**

Ph D, Mineral and Energy Resource Economics, West Virginia State University, USA, 1984, retired from the post of Senior Researcher, Mineral and Coal Technology R&D Center, Agency for Energy and Mineral Research, Ministry of Energy and Mineral Resources, Indonesia.

### **Dr. Samy Khalaf Allah Ibrahim**

PhD of Irrigation &Hydraulics Engineering, 01/2012 under the title of: "Groundwater Management under Different Development Plans in Farafra Oasis, Western Desert, Egypt".

### **Dr. Ahmet ÇİFCİ**

Ph.D. in Electrical Engineering, Currently Serving as Head of Department, Burdur Mehmet Akif Ersoy University, Faculty of Engineering and Architecture, Department of Electrical Engineering.

## **Dr. M. Varatha Vijayan**

Annauniversity Rank Holder, Commissioned Officer Indian Navy, Ncc Navy Officer (Ex-Serviceman Navy), Best Researcher Awardee, Best Publication Awardee, Tamilnadu Best Innovation & Social Service Awardee From Lions Club.

## **Dr. Mohamed Abdel Fatah Ashabrawy Moustafa**

PhD. in Computer Science - Faculty of Science - Suez Canal University University, 2010, Egypt.

Assistant Professor Computer Science, Prince Sattam bin AbdulAziz University ALkharj, KSA.

## **Prof.S.Balamurugan**

Dr S. Balamurugan is the Head of Research and Development, Quants IS & CS, India. He has authored/co-authored 35 books, 200+ publications in various international journals and conferences and 6 patents to his credit. He was awarded with Three Post-Doctoral Degrees - Doctor of Science (D.Sc.) degree and Two Doctor of Letters (D.Litt) degrees for his significant contribution to research and development in Engineering.

## **Dr. Mahdi Hosseini**

Dr. Mahdi did his Pre-University (12<sup>th</sup>) in Mathematical Science. Later he received his Bachelor of Engineering with Distinction in Civil Engineering and later he Received both M.Tech. and Ph.D. Degree in Structural Engineering with Grade "A" First Class with Distinction.

## **Dr. Anil Lamba**

Practice Head – Cyber Security, EXL Services Inc., New Jersey USA.

Dr. Anil Lamba is a researcher, an innovator, and an influencer with proven success in spearheading Strategic Information Security Initiatives and Large-scale IT Infrastructure projects across industry verticals. He has helped bring about a profound shift in cybersecurity defense. Throughout his career, he has parlayed his extensive background in security and a deep knowledge to help organizations build and implement strategic cybersecurity solutions. His published researches and conference papers has led to many thought provoking examples for augmenting better security.

## **Dr. Ali İhsan KAYA**

Currently working as Associate Professor in Mehmet Akif Ersoy University, Turkey.

**Research Area:** Civil Engineering - Building Material - Insulation Materials Applications, Chemistry - Physical Chemistry – Composites.

## **Dr. Parsa Heydarpour**

Ph.D. in Structural Engineering from George Washington University (Jan 2018), GPA=4.00.

## **Dr. Heba Mahmoud Mohamed Afify**

Ph.D degree of philosophy in Biomedical Engineering, Cairo University, Egypt worked as Assistant Professor at MTI University.

## **Dr. Aurora Angela Pisano**

Ph.D. in Civil Engineering, Currently Serving as Associate Professor of Solid and Structural Mechanics (scientific discipline area nationally denoted as ICAR/08—"Scienza delle Costruzioni"), University Mediterranea of Reggio Calabria, Italy.

## **Dr. Faizullah Mahar**

Associate Professor in Department of Electrical Engineering, Balochistan University Engineering & Technology Khuzdar. He is PhD (Electronic Engineering) from IQRA University, Defense View, Karachi, Pakistan.

## **Prof. Viviane Barrozo da Silva**

Graduated in Physics from the Federal University of Paraná (1997), graduated in Electrical Engineering from the Federal University of Rio Grande do Sul - UFRGS (2008), and master's degree in Physics from the Federal University of Rio Grande do Sul (2001).

## **Dr. S. Kannadhasan**

Ph.D (Smart Antennas), M.E (Communication Systems), M.B.A (Human Resources).

## **Dr. Christo Ananth**

Ph.D. Co-operative Networks, M.E. Applied Electronics, B.E Electronics & Communication Engineering Working as Associate Professor, Lecturer and Faculty Advisor/ Department of Electronics & Communication Engineering in Francis Xavier Engineering College, Tirunelveli.

## **Dr. S.R.Boselin Prabhu**

Ph.D, Wireless Sensor Networks, M.E. Network Engineering, Excellent Professional Achievement Award Winner from Society of Professional Engineers Biography Included in Marquis Who's Who in the World (Academic Year 2015 and 2016). Currently Serving as Assistant Professor in the department of ECE in SVS College of Engineering, Coimbatore.

## **Dr. PAUL P MATHAI**

Dr. Paul P Mathai received his Bachelor's degree in Computer Science and Engineering from University of Madras, India. Then he obtained his Master's degree in Computer and Information Technology from Manonmanium Sundaranar University, India. In 2018, he received his Doctor of Philosophy in Computer Science and Engineering from Noorul Islam Centre for Higher Education, Kanyakumari, India.

## **Dr. M. Ramesh Kumar**

Ph.D (Computer Science and Engineering), M.E (Computer Science and Engineering).

Currently working as Associate Professor in VSB College of Engineering Technical Campus, Coimbatore.

## **Dr. Maheshwar Shrestha**

Postdoctoral Research Fellow in DEPT. OF ELE ENGG & COMP SCI, SDSU, Brookings, SD Ph.D, M.Sc. in Electrical Engineering from SOUTH DAKOTA STATE UNIVERSITY, Brookings, SD.

## **Dr. D. Amaranatha Reddy**

Ph.D. (Postdoctoral Fellow, Pusan National University, South Korea), M.Sc., B.Sc. : Physics.

## **Dr. Dibya Prakash Rai**

Post Doctoral Fellow (PDF), M.Sc., B.Sc., Working as Assistant Professor in Department of Physics in Pachhungga University College, Mizoram, India.

## **Dr. Pankaj Kumar Pal**

Ph.D R/S, ECE Deptt., IIT-Roorkee.

## **Dr. P. Thangam**

PhD in Information & Communication Engineering, ME (CSE), BE (Computer Hardware & Software), currently serving as Associate Professor in the Department of Computer Science and Engineering of Coimbatore Institute of Engineering and Technology.

## **Dr. Pradeep K. Sharma**

PhD., M.Phil, M.Sc, B.Sc, in Physics, MBA in System Management, Presently working as Provost and Associate Professor & Head of Department for Physics in University of Engineering & Management, Jaipur.

## **Dr. R. Devi Priya**

Ph.D (CSE), Anna University Chennai in 2013, M.E, B.E (CSE) from Kongu Engineering College, currently working in the Department of Computer Science and Engineering in Kongu Engineering College, Tamil Nadu, India.

## **Dr. Sandeep**

Post-doctoral fellow, Principal Investigator, Young Scientist Scheme Project (DST-SERB), Department of Physics, Mizoram University, Aizawl Mizoram, India- 796001.

## **Dr. Roberto Volpe**

Faculty of Engineering and Architecture, Università degli Studi di Enna "Kore", Cittadella Universitaria, 94100 – Enna (IT).

## **Dr. S. Kannadhasan**

Ph.D (Smart Antennas), M.E (Communication Systems), M.B.A (Human Resources).

**Research Area:** Engineering Physics, Electromagnetic Field Theory, Electronic Material and Processes, Wireless Communications.

## **Mr. Amit Kumar**

Amit Kumar is associated as a Researcher with the Department of Computer Science, College of Information Science and Technology, Nanjing Forestry University, Nanjing, China since 2009. He is working as a State Representative (HP), Spoken Tutorial Project, IIT Bombay promoting and integrating ICT in Literacy through Free and Open Source Software under National Mission on Education through ICT (NMEICT) of MHRD, Govt. of India; in the state of Himachal Pradesh, India.

## **Mr. Tanvir Singh**

Tanvir Singh is acting as Outreach Officer (Punjab and J&K) for MHRD Govt. of India Project: Spoken Tutorial - IIT Bombay fostering IT Literacy through Open Source Technology under National Mission on Education through ICT (NMEICT). He is also acting as Research Associate since 2010 with Nanjing Forestry University, Nanjing, Jiangsu, China in the field of Social and Environmental Sustainability.

## **Mr. Abilash**

M.Tech in VLSI, BTech in Electronics & Telecommunication engineering through A.M.I.E.T.E from Central Electronics Engineering Research Institute (C.E.E.R.I) Pilani, Industrial Electronics from ATI-EPI Hyderabad, IEEE course in Mechatronics, CSHAM from Birla Institute Of Professional Studies.

## **Mr. Varun Shukla**

M.Tech in ECE from RGPV (Awarded with silver Medal By President of India), Assistant Professor, Dept. of ECE, PSIT, Kanpur.

## **Mr. Shrikant Harle**

Presently working as a Assistant Professor in Civil Engineering field of Prof. Ram Meghe College of Engineering and Management, Amravati. He was Senior Design Engineer (Larsen & Toubro Limited, India).

## **Zairi Ismael Rizman**

Senior Lecturer, Faculty of Electrical Engineering, Universiti Teknologi MARA (UiTM) (Terengganu) Malaysia Master (Science) in Microelectronics (2005), Universiti Kebangsaan Malaysia (UKM), Malaysia. Bachelor (Hons.) and Diploma in Electrical Engineering (Communication) (2002), UiTM Shah Alam, Malaysia.

## **Mr. Ronak**

**Qualification:** M.Tech. in Mechanical Engineering (CAD/CAM), B.E.

Presently working as a Assistant Professor in Mechanical Engineering in ITM Vocational University, Vadodara. Mr. Ronak also worked as Design Engineer at Finstern Engineering Private Limited, Makarpura, Vadodara.

# Table of Contents

Volume-9, Issue-11, November 2023

S. No	Title	Page No.
1	<b>Current Use of Natural Gas within the European Union</b> Authors: Ľubomíra Kmeťová  DOI: <a href="https://dx.doi.org/10.5281/zenodo.10219939">https://dx.doi.org/10.5281/zenodo.10219939</a>  <b>DIN</b> Digital Identification Number: IJOER-NOV-2023-3	01-05
2	<b>Design of an Experimental Device for the Analysis of the Influence of Sound Waves on the CPU Cooling Process - Part II</b> Authors: Lukáš Tóth, Romana Dobáková  DOI: <a href="https://dx.doi.org/10.5281/zenodo.10219994">https://dx.doi.org/10.5281/zenodo.10219994</a>  <b>DIN</b> Digital Identification Number: IJOER-NOV-2023-4	06-10
3	<b>Structural Design of Atypical Metal hydride Tank and Investigation of Generated Temperature Fields: Part II</b> Authors: Filip Duda, Natália Jasminská, Peter Milenovský  DOI: <a href="https://dx.doi.org/10.5281/zenodo.10220037">https://dx.doi.org/10.5281/zenodo.10220037</a>  <b>DIN</b> Digital Identification Number: IJOER-NOV-2023-5	11-16
4	<b>Design of a Model of Liquid Feeder to an Incinerator of Hazardous Waste and its Optimization from the Cooling Point of View: Part II</b> Authors: Ivan Mihálik, Marián Lázár, Tomáš Brestovič, Peter Milenovský  DOI: <a href="https://dx.doi.org/10.5281/zenodo.10220069">https://dx.doi.org/10.5281/zenodo.10220069</a>  <b>DIN</b> Digital Identification Number: IJOER-NOV-2023-6	17-22
5	<b>Liquid Impact Sheet Metal Deformation of Superni (Inconel) 718 using Inclined Edge (Conical) DIE</b> Authors: E. Hazya, Dr S Gajanana, Dr. P. Laxminarayana  DOI: <a href="https://dx.doi.org/10.5281/zenodo.10220168">https://dx.doi.org/10.5281/zenodo.10220168</a>  <b>DIN</b> Digital Identification Number: IJOER-NOV-2023-7	23-28
6	<b>Use of Peltier Cells in the Cooling Process</b> Authors: Romana Dobáková, Lukáš Tóth, Tomáš Brestovič  DOI: <a href="https://dx.doi.org/10.5281/zenodo.10220217">https://dx.doi.org/10.5281/zenodo.10220217</a>  <b>DIN</b> Digital Identification Number: IJOER-NOV-2023-8	29-34-

# Current Use of Natural Gas within the European Union

Ľubomíra Kmeťová

<sup>1</sup>Department of Power Engineering, Faculty of Mechanical Engineering, Technical University of Košice, Slovakia

\*Corresponding Author

Received: 01 November 2023/ Revised: 11 November 2023/ Accepted: 20 November 2023/ Published: 30-11-2023  
Copyright © 2023 International Journal of Engineering Research and Science

This is an Open-Access article distributed under the terms of the Creative Commons Attribution Non-Commercial License (<https://creativecommons.org/licenses/by-nc/4.0>) which permits unrestricted Non-commercial use, distribution, and reproduction in any medium, provided the original work is properly cited.

**Abstract**— In connection with the heated political situation to the east of the European Union (EU) borders, there is a growing interest in the discovery of new reserves of natural gas or new suppliers of this fossil fuel. The following article discusses the current suppliers of natural gas to the EU, the energy self-sufficiency of the EU and the possibility of transporting natural gas in the form of LNG.

**Keywords**— natural gas, REPowerEU plan, liquefied natural gas (LNG), H2 pilot project, floating storage of natural gas.

## I. INTRODUCTION

The current political situation requires new and unconventional ways of solving the storage and transportation of natural gas in large quantities and over long distances.

## II. CURRENT NATURAL GAS SUPPLIES TO THE EUROPEAN UNION

In response to the difficulties and disruption of the global energy market caused by Russia's invasion of Ukraine, the European Commission started implementing the REPowerEU plan in May 2022. Thanks to the REPowerEU plan, the states of the European Union succeed in diversifying their energy supplies, especially [1]:

- Conclusion of agreements with other third countries on the import of gas through the gas pipeline,
- Investment in the joint purchase of liquefied natural gas (Fig. 1),
- Securing strategic partnerships with Namibia, Egypt, and Kazakhstan to guarantee safe and sustainable supplies of clean hydrogen,
- Signing of agreements with Egypt and Israel on the import of natural gas to Europe



FIGURE 1: Transportation of LNG by tanker [2]

Most natural gas supplies to the EU are currently routed via pipelines from Norway and tankers from the US in the form of LNG. In the summer, the key supplies were mainly liquefied natural gas (LNG) by sea and pipeline gas from Norway (Fig. 2).

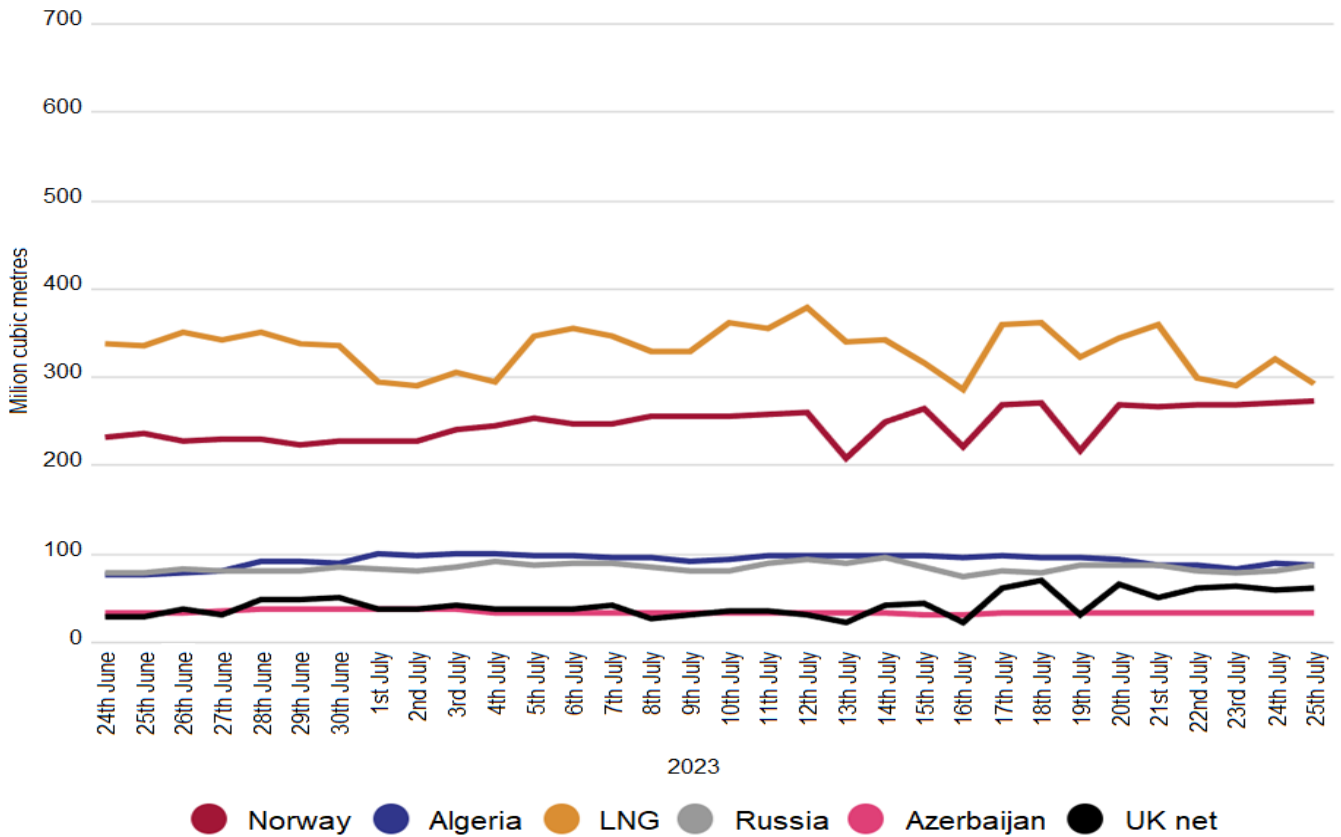


FIGURE 2: Daily NG supplies to EU countries in cubic metres (from 24<sup>th</sup> of June to 25<sup>th</sup> of July 2023) [3]

### III. ENERGY SELF-SUFFICIENCY OF THE EU

There is no miracle solution that could reduce the EU's dependence on the import of natural gas from Russia. It was possible to achieve a gradual reduction of gas imports from Gazprom by combining various approaches and solutions.

According to the Europe Gas Tracker Report 2022, infrastructure investments amounting to EUR 48.5 billion are needed for the complete replacement of Russian gas with LNG. Of this, 12.3 billion are costs for the completion of terminals and 36.3 billion are costs for the completion of networks. It is already evident from these figures that a full replacement is not possible in the foreseeable future.

In March 2023, the EU tightened its rules to increase the capacity of energy from renewable sources. The binding EU target by 2030 has thus increased to 42.5 % with the ambition to reach 45%. This would almost double the share of renewable energy in the EU.

The European gas industry is trying to green the molecules of transported gases. Bio or synthetic methane are comparable in properties to natural gas.

However, hydrogen, potentially a much more significant player in the field of renewable and low-emission gases, presents far greater challenges for the traditional gas industry due to its different physical and chemical properties.

Ongoing initiatives in Europe have the common goal of establishing a maximum safe limit for the volume percentage of hydrogen in the mixture distributed with natural gas (20 – 30 % vol). The reason is to maximize the use of hydrogen from renewable sources without further treatment, as a substitute for fossil natural gas.

When replacing natural gas with other renewable sources, one of the goals of the European Union is to produce 35 billion cubic meters of biomethane by 2030 in Europe. This would correspond to roughly 10 to 12 percent of annual consumption. Through the supply of bio CNG and bio-LNG, it will be possible to significantly decarbonize, for example, public transport.

The hydrogen should also have a significant impact on the decarbonisation of the EU – it is mainly green hydrogen, which is produced from energy from renewable sources through the electrolysis of water.

From the point of view of the gas industry, the biggest challenge is the preparation and adaptation of the gas infrastructure for hydrogen. Because it is three times lighter than methane, which is the main component of natural gas.

Last year, a project called H2pilot took place in the Slovak Republic. It is a project of testing the mixing of 10 % hydrogen into natural gas in the Slovak village (Blatná na Ostrove).



**FIGURE 3: H2 Pilot - DSO 10% Hydrogen blending project in Slovakia [6]**

#### IV. LIQUEFIED NATURAL GAS

Liquefied natural gas, or LNG, is natural gas that has been converted into liquid form for ease of storage or transportation by cooling the natural gas to approximately  $-162^{\circ}\text{C}$ . It is then stored at atmospheric pressure. Liquefied natural gas is transported by tankers to national gas transmission systems and then through distribution pipelines to consumers.

LNG occupies approximately 600 times less volume than gaseous natural gas, which is its main advantage for storage and transport. LNG is made up of 90 – 100 % methane and, depending on the mining area, also contains residues of ethane, propane, higher hydrocarbons, nitrogen, and other gases. Its calorific value is around 55 MJ per kg, expressed in litres it is about 22 MJ per liter. The flash point of LNG is  $540^{\circ}\text{C}$ . Before the natural gas is liquefied, it is necessary to remove the undesirable components. The permissible amounts of these undesirable components are shown in tab. 1.

**TABLE 1  
PERMISSIBLE AMOUNTS OF UNDESIRABLE COMPONENTS IN LNG [7]**

Component	Unit	Maximum permissible amount
Water	ppm vol. <sup>*1</sup>	1
Carbon dioxide	ppm vol.	1000
Sulfur compounds	mg/Nm <sup>3</sup> <sup>*2</sup>	30
Mercury	mg/Nm <sup>3</sup>	10
Aromatic hydrocarbons	ppm vol.	10

<sup>\*1</sup> ppm vol. means one volume part per million,

<sup>\*2</sup> mg/Nm<sup>3</sup> means milligram per normal cubic meter (under normal conditions – 101 325 Pa and 0 °C)

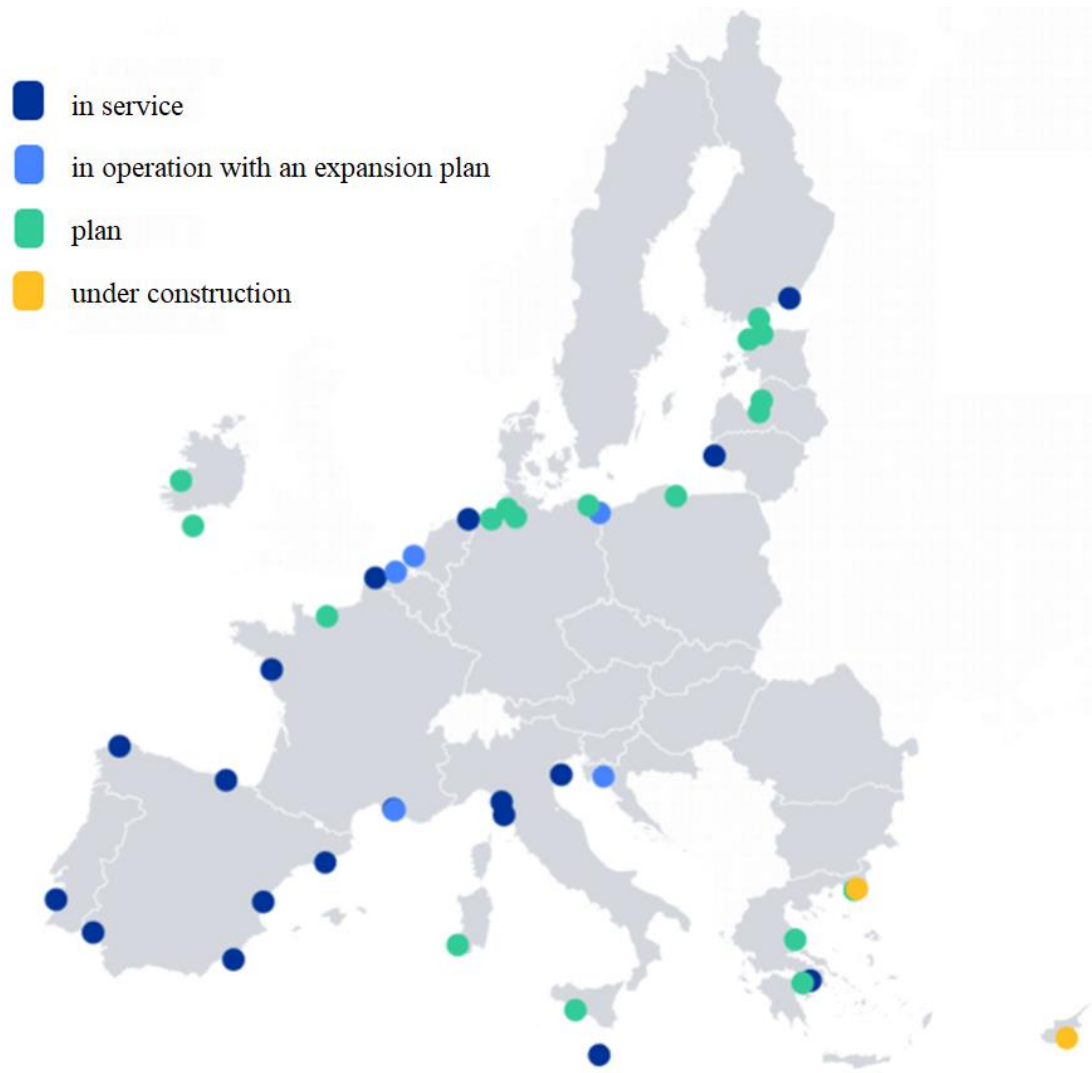


**FIGURE 4: LNG infrastructure in the European Union [8]**

The largest ship for transporting liquefied natural gas was presented at the end of April this year in Shanghai, China. The developer of the vessel is the Chinese company Jiangnan Shipyard. The vessel has a transport capacity of 93,000 cubic meters of raw material.

The ship named Harzand is 230 meters long and 36.6 meters wide. Harzand is fuelled by liquefied petroleum gas (LPG) and is supposed to meet the latest greenhouse gas emission regulations [9].

Large-capacity LNG terminals (Fig. 5) are located on the coast or as floating facilities (Floating Storage and Regasification Units - FSRU), which enable the arrival of LNG tankers and subsequently transform LNG into natural gas.

Importing liquefied natural gas is a way to diversify the suppliers and routes the EU uses to obtain natural gas.

In the first half of 2022, the United States became the largest supplier of LNG to the EU, covering almost 50 % of total imports. The import of LNG from the USA has more than doubled year-on-year.

The total capacity of the EU to import LNG is considerable (approximately 157 billion m<sup>3</sup> per year in the form of liquefied gas re-converted to a gaseous state) - enough to meet approximately 40% of the total demand for gas. However, access to LNG infrastructure is uneven within the EU [8].

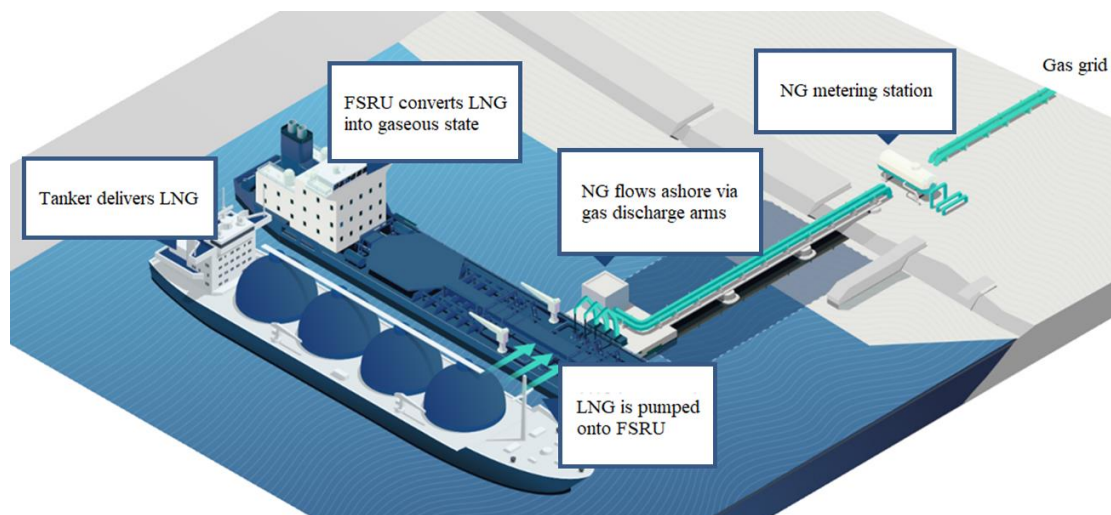


**FIGURE 5: Floating Storage and Regasification Unit (FSRU) [10]**

## V. CONCLUSION

Natural gas is a fossil fuel. Although its combustion produces significantly fewer CO<sub>2</sub> emissions than, for example, in coal-fired power plants. However, during the extraction and transportation of natural gas, a much more dangerous greenhouse gas, methane, is released.

The latest summary report of the International Panel on Climate Change warns that to keep global warming within safe limits, it is necessary to stop any new investment in fossil fuel projects.

## ACKNOWLEDGMENTS

This paper was written with financial support from the VEGA granting agency within the projects no. 1/0224/23 and no. 1/0532/22, from the KEGA granting agency within the project no. 012TUKE-4/2022 and with financial support from the APVV granting agency within the projects no. APVV-15-0202, no. APVV-20-0205 and no. APVV-21-0274.

## REFERENCES

- [1] EUROPEAN COMMISSION. Communication from the Commission to the European Parliament, the European Council, the Council, the European Economic and Social Committee and the Committee of the Regions. REPowerEU Plan. Brussels. 18.05.2022. <<https://eur-lex.europa.eu/legal-content/EN/TXT/?uri=COM%3A2022%3A230%3AFIN&qid=1653033742483>>. (Accessed 08.09.2023)
- [2] A liquefied natural gas (LNG) tanker is tugged towards a thermal power station in Futtsu, east of Tokyo, Japan. 13.11.2017. REUTERS/Issei Kato. Public:
- [3] <<https://www.reuters.com/business/energy/japan-facilitate-lng-allocation-across-power-gas-industries-event-emergency-2022-10-17/>>. (Accessed 08.09.2023)
- [4] BRUEGEL. European natural gas imports. 27.7.2023. <<https://www.bruegel.org/dataset/european-natural-gas-imports>>. (Accessed 08.09.2023)
- [5] EUROPEAN COMMISSION. Renewable energy targets. Public: <[https://energy.ec.europa.eu/topics/renewable-energy/renewable-energy-directive-targets-and-rules/renewable-energy-targets\\_en](https://energy.ec.europa.eu/topics/renewable-energy/renewable-energy-directive-targets-and-rules/renewable-energy-targets_en)>. (Accessed: 08.09.2023)
- [6] European Commission and industry leaders launch Biomethane Industrial Partnership. Brussels, 22.09.2022. <[https://commission.europa.eu/news/european-commission-and-industry-leaders-launch-biomethane-industrial-partnership-2022-09-28\\_en](https://commission.europa.eu/news/european-commission-and-industry-leaders-launch-biomethane-industrial-partnership-2022-09-28_en)>. (Accessed 08.09.2023)
- [7] H2 Pilot – DSO 10% Hydrogen blending project. Public: <<https://www.spp-distribucia.sk/o-spolocnosti/co-robime/h2-pilot/>>. (Accessed 08.09.2023)
- [8] Liquefied natural gas. 19.05.2015. Public: <<https://oenergetice.cz/plyn/zkapalneny-zemni-plyn-lng>>. (Accessed 08.09.2023)
- [9] Infographic – Liquefied natural gas infrastructure in the EU. <<https://www.consilium.europa.eu/sk/infographics/lng-infrastructure-in-the-eu>>. (Accessed 08.09.2023)
- [10] China Daily. World's biggest ship for gas transport unveiled. 26.04.2023. <<https://www.chinadaily.com.cn/a/202304/26/WS64487c98a310b6054facfcd.html>>. (Accessed 08.09.2023)
- [11] Floating Storage and Regasification Unit. Public: <<https://www.rwe.com/-/media/RWE/images/11-forschung-und-entwicklung/projektvorhaben/lng-schwimmende-terminals/rwe-infographic-floating-lng-terminal.jpg>>. (Accessed 08.09.2023)
- [12] DOBÁKOVÁ, R., JASMINSKÁ, N., KMEŤOVÁ, L., LÁZÁR, M. Plynárenské zariadenia. 1st. Edition. Košice: Technical University of Košice. 2022. 266 p. [CD-ROM]. ISBN 978-80-553-4165-1.

# Design of an Experimental Device for the Analysis of the Influence of Sound Waves on the CPU Cooling Process - Part II

Lukáš Tóth<sup>1\*</sup>, Romana Dobáková<sup>2</sup>

Department of Energy Engineering, Faculty of Mechanical Engineering, Technical University of Košice, Slovakia

\*Corresponding Author

Received: 01 November 2023/ Revised: 10 November 2023/ Accepted: 18 November 2023/ Published: 30-11-2023

Copyright © 2023 International Journal of Engineering Research and Science

This is an Open-Access article distributed under the terms of the Creative Commons Attribution

Non-Commercial License (<https://creativecommons.org/licenses/by-nc/4.0>) which permits unrestricted

Non-commercial use, distribution, and reproduction in any medium, provided the original work is properly cited.

**Abstract**— The article describes the calibration procedures and the creation of a series of initial data packages as a basis for comparative experiments in the process of increasing the efficiency of CPU air cooling in the case of commonly available types of coolers. It then describes the course of the experiment, the input parameters and the data obtained from the calibration of the basic model at different power settings of the fan mounted on the DeepCool AG200 air cooler. The output of the article is a model of cooling performance based on fan speeds and ambient operating temperature.

**Keywords**— CPU, TDP, cooling process.

## I. INTRODUCTION

With the development of CPUs and with the annual increase in their computing power, there is also an increase in the amount of heat generated during their operation. The heat generated during CPU operation is one of the limiting factors of their maximum computing performance. To remove heat from the surface of the CPU, various methods were gradually introduced, from passive aluminium coolers to coolers with forced air flow provided by a fan, to water circuits that transport the generated heat using a heat-carrying medium to larger coolers located outside the CPU area, where the heat is removed to surroundings. Increasing the area of water coolers results in taking up larger areas on the computer case. This procedure of enlarging the heat exchange surface is unsuitable for portable PCs. For this reason, there has recently been a re-development of air coolers with heat pipes, where there is an effort to increase their performance using methods of disrupting the boundary layer of the flowing air in the ribs, to increase the removal of heat to the surroundings.

## II. THEORETICAL FOUNDATION OF THE CALIBRATION MODEL

To create a suitable calibration model, against which it would be possible to relate the results of experiments for disruption of the boundary layer of flowing air, it is necessary to create a package of comparative data. As the basis of the experiment described in the previous article, a block of aluminium with dimensions of 85x58x16 mm was used, in which there are 3 heat sources with a total joint power of 150W, which simulated the operation of the CPU. Thermometers are placed in the volume of the aluminium block and on its surface to determine the average temperature of this block at different power settings of the heating elements and the cooler. A DeepCool AG200 air cooler with a total cooling capacity of TDP 100W is placed on the surface of one of the largest surfaces.

In the design of the experiment, a cooling performance measurement system was used at different power settings of the fan given by its speed. The amount of heat that needed to be removed was determined by the voltage and current supplied to the heating elements. If we know the voltage and current supplied to the heating elements, we can determine the heat output dissipated by the cooler to the environment at the point, when the temperature of the aluminium block stabilizes. Due to the insulation used, we can neglect the removal of heat to the surroundings in other ways than cooling with the use of a cooler. By changing the speed of the fan, the amount of air that passed through the heat exchange plates of the radiator changed and thus also the amount of energy that was transferred to the air. At each setting of the speed and the amount of heat supplied by the heating bodies, the temperature of the aluminium block stabilized, where the amount of heat supplied to the body was equal to the amount of heat removed, as shown in Figure 1.

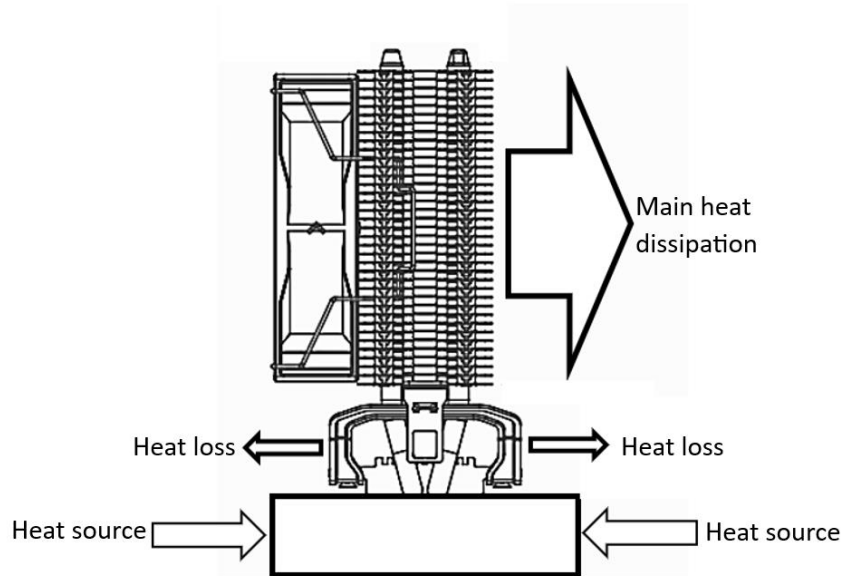


**FIGURE 1: Temperature flow through the experimental device**

### III. BOUNDARY CONDITIONS

Due to the simple possibility of observing and comparing changes during individual experimental modifications of the cooling device, it is necessary to maintain the same boundary conditions during the entire duration of the experiment. One of the main boundary conditions that can have a significant impact on the obtained data is the ambient temperature. When the ambient temperature changes, there is a change in the temperature differential between the heat exchange surfaces and the flowing air and the parameters associated with the heat flow. This will subsequently cause an increase or reducing the cooling performance of the device. To eliminate these undesirable effects, it is necessary to perform a partially idealized experiment. The device is in an open room with a floor area of 3x8 m, in which the temperature is maintained at 22°C. Considering the size of the room and the relatively small heating power of the experimental equipment, it is possible to assume that the temperature in the room is stable. In the case of placing the experimental device in a computer case, as it is commonly used, there would be significant temperature fluctuations during the experiment and the need to create conversion coefficients relating to the actual temperature in a small space.

An important boundary condition for the possibility of comparing different power settings of the fan, or the influence of elements to increase the cooling efficiency, is the possibility of a stable setting of the heat flow that the cooler is supposed to remove. For this purpose, a laboratory source with adjustable voltage and current output was used. With the ability to accurately regulate and record voltage and current, it is possible to accurately reproduce the heat output delivered to the heated block of aluminium that represents the simulated CPU.

The last condition for the reproducibility of the created calibration model is the possibility of regulating the fan speed. The original fan supplied by the manufacturer of the DeepCool AG200 cooling device is connected to a laboratory power supply that regulates the supplied voltage, which controls the speed of the fan. The speed of rotation is recorded using a recording device that is connected to a digital tachometer built directly into the fan. Thanks to the connection between voltage and revolutions, it is then possible to easily regulate the speed of rotation of the fan based on the change in voltage without the need to detect the current revolutions.

### IV. PROCEDURE OF MEASUREMENTS AND EVALUATION OF RESULTS

An Arduino MEGA microcontroller was used to record the measured data, which then sent the obtained and processed data to the computer. Dallas DS18B20 digital sensors on the surface in the number of 7 pieces and 3 pieces of NTC 10k thermistors in the core of the aluminium block were used to record the temperatures. Temperature data was recorded approximately every second and then these temperature values were averaged. Averaging temperatures enabled a better comparison of measured data and prevented inaccuracies caused by local heating of one of the thermometers.

To determine the efficiency of cooling the aluminium block using air cooling, a system of comparison of the maximum temperatures achieved at precisely defined heat outputs of heating elements and fan speeds while maintaining the same value of the ambient temperature was used. A gradual increase in the power of the heating elements was carried out according to the selected schedule, always after reaching a stabilized temperature of the aluminium block at the specified fan speed. The measured data subsequently created a table of dependences of the maximum temperatures achieved with respect to the fan speed and the power of the heating elements.

Increasing the thermal output of the heating elements was carried out by changing the voltage and current values on the laboratory power source. In tab. 1 shows the measured maximum stabilized temperatures of the aluminium block with respect to the heat output supplied to the aluminium block and the speed of the fan.

**TABLE 1**  
**DEVELOPMENT OF TEMPERATURES DEPENDING ON THE SPEED OF THE FAN AND THE HEAT OUTPUT OF THE HEATING ELEMENTS**

	Thermal performance	9W	16W	24W	36,6W	49,7W	64W	81W	99W
		Temperature (°C)							
Fan speed	1450 rpm	27,12	29,73	33,43	39,13	44,96	50,92	58,46	66,89
	1750 rpm	26,142	29,31	33,1	38,32	43,96	49,78	57,32	65,41
	2100 rpm	26,04	29,05	32,36	37,41	42,84	48,53	55,71	63,27
	2325 rpm	25,88	28,73	32,15	36,62	41,74	47,45	54,46	61,61
	2575 rpm	25,64	28,59	31,93	36,40	41,50	46,92	53,84	60,71
	2800 rpm	25,74	28,38	31,62	36,29	41,26	46,52	52,94	59,84

The course of measurements was carried out at an ambient temperature of  $22^{\circ}\text{C} \pm 0.5^{\circ}\text{C}$ . From table 1 and fig. 2 there is a linear change in temperature with respect to the change in fan speed and heat output. According to the assumption, with increasing revolutions, the average and maximum temperature of the aluminium block decreased due to the increasing cooling power, which increased with the increase in the speed of rotation of the fan and thus also with the increase in the volumetric flow of cooling air. The increase in fan speed was realized by increasing the supply voltage by 1V at each measuring step.

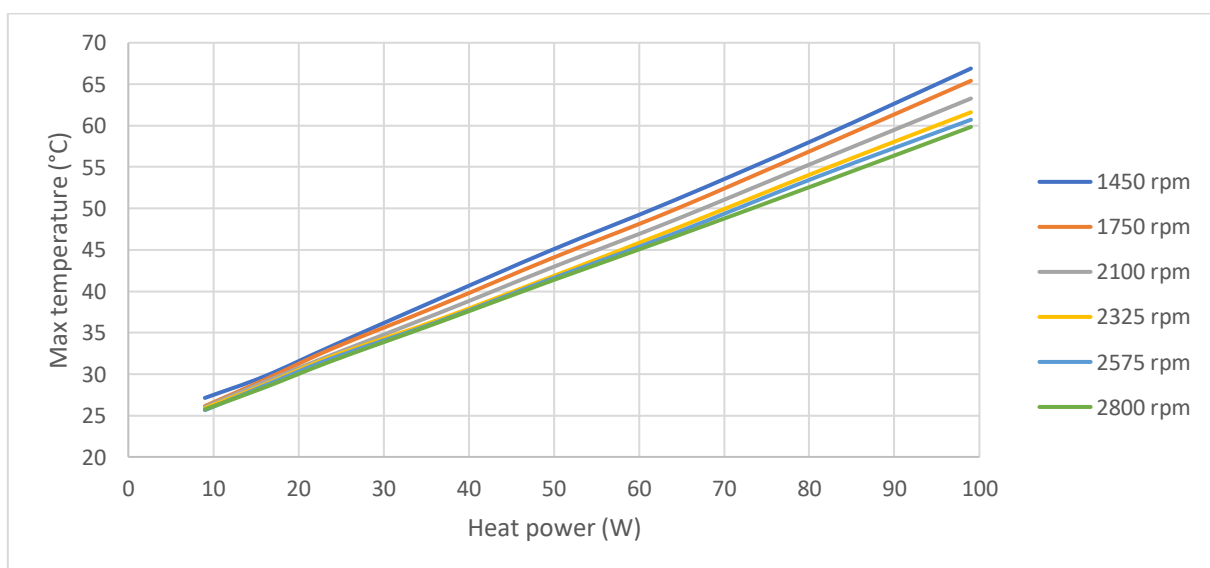


**FIGURE 2: Dependence of the temperature change on the heat output of the heating elements and fan speed**

If only the maximum heat output of 99 W and the effect of the change in speed on the maximum temperature reached in the aluminium block were monitored, it would be possible to determine a linear temperature drop with respect to the fan rotation speed. A change in speed will cause a change in the speed of air flow through the body of the cooler, which will also increase the amount of heat transferred to the environment while maintaining the same temperature difference between the air inlet and outlet. The linear decrease in temperature is shown in fig. 3.

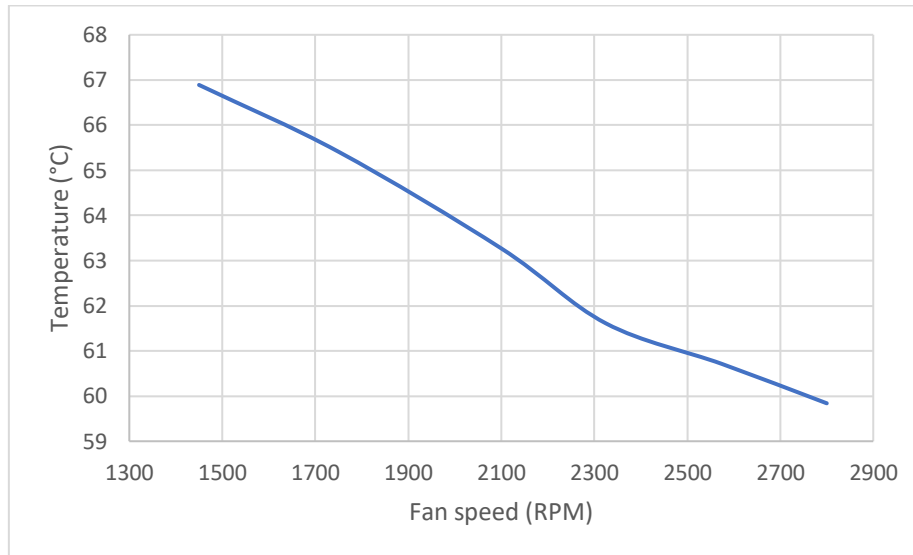


**FIGURE 3: Change in the maximum temperature reached with a change in fan speed**

During the experimental measurements, a recording was made of the overall course of temperature change and subsequent stabilization. Due to different powers and stabilization times, the data set was modified and shown in fig. 4.

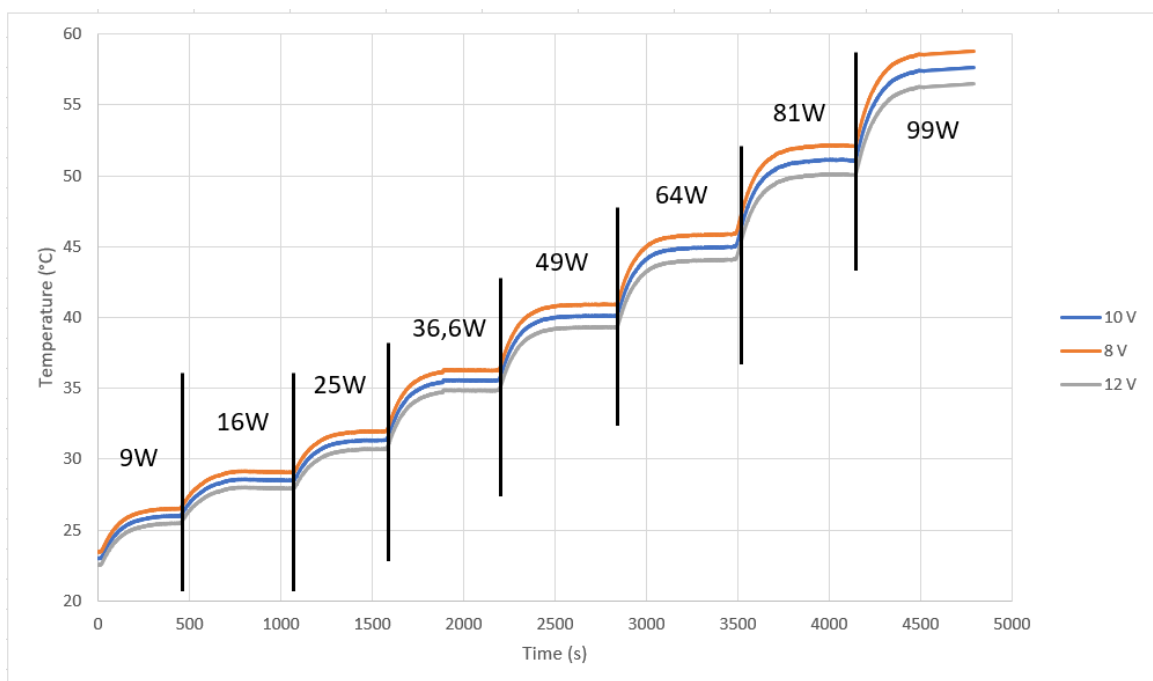


**FIGURE 4: Change in maximum temperature with different heat outputs of heating elements and fan speed over time**

As can be seen from the given dependence, there is a significant decrease in the maximum reached temperature of the aluminium block with respect to the speed of the fan. From the obtained data forming the comparison package, it is possible to predict the resulting maximum temperature at known fan speed and ambient temperature at the specified thermal performance of the heating elements (simulated CPU).

## V. CONCLUSION

The creation of a comparison and calibration model is an essential basis when dealing with increasing the efficiency of CPU cooling using air cooling devices. Without the creation of a reliable comparative model against which it would be possible to relate the results measured during the process of increasing the efficiency under different operating conditions, it is not possible to accurately determine the change in cooling performance due to the use of innovative methods of increasing the cooling performance.

## ACKNOWLEDGEMENTS

This paper was written with the financial support from the VEGA granting agency within the Projects No. 1/0224/23 and No. 1/0532/22, from the KEGA granting agency within the Project No. 012TUKE-4/2022, and with the financial support from the APVV granting agency within the Projects No. APVV-15-0202, APVV-20-0205 and APVV-21-0274.

## REFERENCES

- [1] Siricharoenpanich, A., Wiriyasart, S., Srichat, A., Naphon, P.: *Thermal management system of CPU cooling with a novel short heat pipe cooling system*. Case Studies in Thermal Engineering. 15 (2019), 100545
- [2] Yousefi, T., Mousavi, S.A., Farahbakhsh, B., Saghir, M.Z.: *Experimental investigation on the performance of CPU coolers: Effect of heat pipe inclination angle and the use of nanofluids*. Microelectronics Reliability. Volume 53, Issue 12, (2013) p.1954-1961
- [3] Kim, K.-S., Won, M.-H., Kim, J.-W., Back, B.-J.: *Heat pipe cooling technology for desktop PC CPU*. Applied Thermal Engineering. Volume 23, Issue 9, (2003) p. 1137-1144.
- [4] Li, Ch., Li, J.: *Passive Cooling Solutions for High Power Server CPUs with Pulsating Heat Pipe Technology: Review*. Frontiers in Energy Research. Volume 9 (2021).
- [5] DEEPCOOL. Available on <<https://www.deepcool.com/products/Cooling/cpuaircoolers/AG200-Single-Tower-CPU-Cooler-1700-AM5/2022/16203.shtml>>.
- [6] Cheng, C.C., Chang, P.C., Li, H.C., Hsu, F.I.: *Design of a single-phase immersion cooling system through experimental and numerical analysis*. International Journal of Heat and Mass Transfer. 160 (2020), 120203.
- [7] Liang, K., Li, Z., Chen, M., Jiang, H.: *Comparisons between heat pipe, thermoelectric system, and vapour compression refrigeration system for electronics cooling*. Applied Thermal Engineering. 146 (2019), p. 260-267.
- [8] Qiu, D., Cao, L., Wang, Q., Hou, F., Wang, X.: *Experimental and numerical study of 3D stacked dies under forced air cooling and water immersion cooling*. Microelectronics Reliability. 74 (2017), p. 34-43.

# Structural Design of Atypical Metal hydride Tank and Investigation of Generated Temperature Fields: Part II

Filip Duda<sup>1</sup>, Natália Jasminská<sup>2</sup>, Peter Milenovsky<sup>3</sup>

Department of Power Engineering, Faculty of Mechanical Engineering, Technical University of Košice, 042 00 Košice, Slovak Republic

\*Corresponding Author

Received: 02 November 2023/ Revised: 12 November 2023/ Accepted: 19 November 2023/ Published: 30-11-2023

Copyright © 2023 International Journal of Engineering Research and Science

This is an Open-Access article distributed under the terms of the Creative Commons Attribution

Non-Commercial License (<https://creativecommons.org/licenses/by-nc/4.0>) which permits unrestricted

Non-commercial use, distribution, and reproduction in any medium, provided the original work is properly cited.

**Abstract**— In part 1 of the article, temperature fields generated in a metal hydride tank of an atypical shape were investigated, where the tank was immersed in a cooling liquid. For the total temperature in the storage tank to be reduced even more, it is necessary to design an effective passive heat exchanger system that will remove this generated heat towards the inner wall of the storage tank, where this heat will then be effectively removed by the cooling liquid located on the outside of the storage tank. In part 2 of this article, an internal heat transfer intensifier is designed and subsequent verification of temperature fields using simulation in the ANSYS CFX program.

**Keywords**— Metal hydride, pressure tank, heat transfer.

## I. INTRODUCTION

Hydrogen as a safe, clean, efficient and energy carrier is a suitable candidate for reducing and eliminating greenhouse gas emissions. Hydrogen storage technology, which is one of the key challenges in the development of the hydrogen economy, is being addressed by the continuous efforts of scientists. Progress in hydrogen storage technology research and the latest developments in hydrogen storage materials are recorded. Common storage methods such as high-pressure gas or cryogenic storage cannot meet future storage requirements. Therefore, relatively advanced storage methods such as the use of metal hydrides and organic structure and carbon materials are being developed as promising alternatives. The combination of chemical and physical storage of hydrogen in certain materials has potential advantages among all storage methods. Metal hydrides have been intensively investigated to improve their pressure, hydrogen storage capacity, kinetics, cycle stability and thermal response, which depend on the composition and structural properties of the alloys.

The biggest disadvantage of storing hydrogen in metal hydrides is their weight and the need to create an efficient system for cooling the tank, because during the process of absorbing hydrogen into the structure of the metal alloy, heat is released, which reduces the amount of stored hydrogen and reduces the kinetics of absorption. Therefore, research on the cooling system within this hydrogen storage method is essential.

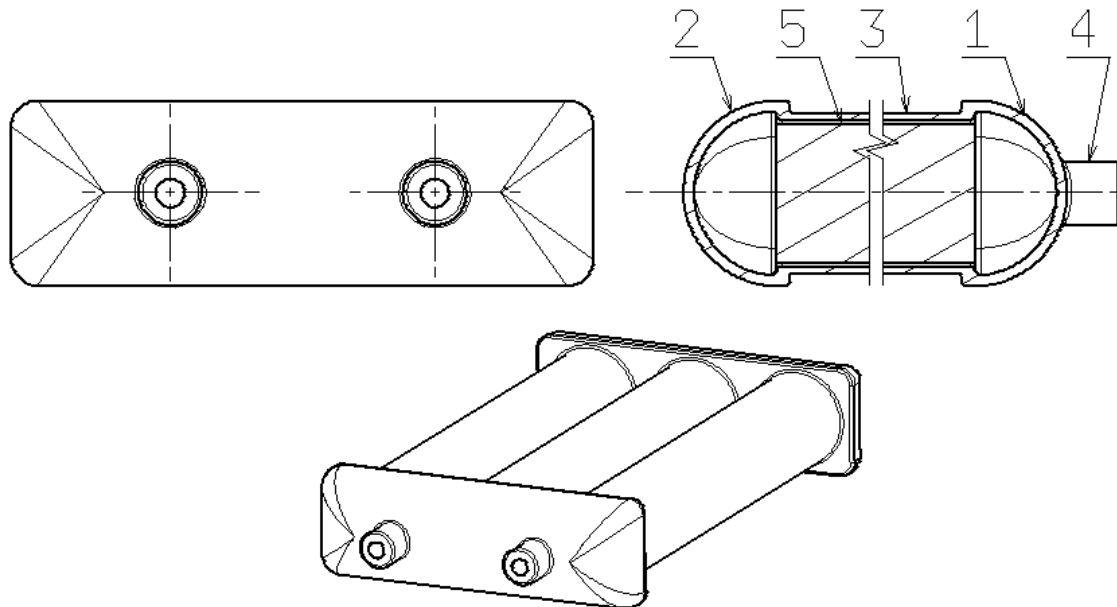
This work deals with the design of a hydrogen storage system in a metal hydride storage tank of an atypical shape with the help of a passive internal heat transfer intensifier, with the help of which the generated heat is removed towards the inner wall of the storage tank, where a storage tank effectively cooled by a cooling liquid is designed.

## II. STRUCTURAL DESIGN OF AN ATYPICAL METAL HYDRIDE STORAGE TANK

The atypical tanks consists of three main parts, namely three cylindrical seamless pipes with a diameter of 60.3 mm with a wall thickness of 2.6 mm, two bottoms of an atypical shape, one of which has two holes with supply of hydrogen to the tank, on the holes there are flanges with a 1/4" NPT thread and inside the cylindrical tubes there are a heat transfer intensifiers for efficient removal of the generated heat to the inner wall of the tank, where the heat is subsequently cooled by the cooling liquid. The seamless pipes and bottoms of the atypical tank are made of 316L-1.4404 steel, where this steel is suitable for hydrogen applications based on the STN EN 13322-2 standard. The material and mechanical properties of the selected steel are shown in TABLE 1.

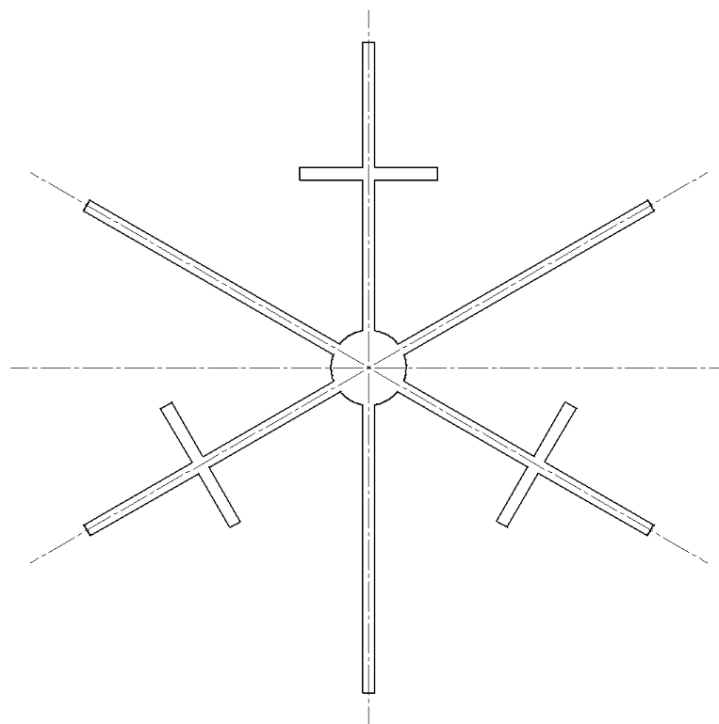
The structural design of the internal heat transfer intensifier consists of three primary ribs on which there are protrusions with a length of 5 mm and a thickness of 1 mm and three secondary ribs with no protrusions. The ribs of the designed intensifier describe a circle with a diameter of 52 mm and thus there is a gap of 1.5 mm to the inner wall of the tank. The intensifier is made of aluminum because it has good thermal conductivity. The heat generated in the metal hydride during the process of hydrogen absorption into its inner structure is approximately 1 MJ per 1 m<sup>3</sup> of stored hydrogen.

FIG 1 shows the structural design of an atypical tank and FIG 2 shows the structural design of the internal heat transfer intensifier.



**FIGURE 1: Structural design of an atypical metal hydride storage tank**

Where: 1- Bottom of atypical shape with two holes for hydrogen supply, 2- Bottom of atypical shape-cap, 3-cylindrical seamless pipes, 4- Flange with 1/4" NPT thread, 5- internal heat transfer intensifier



**FIGURE 2: Structural design of the internal heat transfer intensifier**

**TABLE 1**  
**MECHANICAL PROPERTIES OF STAINLESS STEEL 316 L-1.4404**

0.2% Re (MPa)	Rm (MPa)	$\rho$ (kg·m <sup>-3</sup> )	$\mu$	E (MPa)
205	515	7950	0.3	$2.1 \cdot 10^5$

Where: *Re*-yield strength, *Rm*-strength strength,  $\rho$ -density,  $\mu$ -Poisson's number and *E*-Young's modulus of elasticity.

The operational characteristics of the designed tank with internal heat transfer intensifiers are shown in TABLE 2.

**TABLE 2**  
**OPERATIONAL CHARACTERISTICS OF THE DESIGNED ATYPICAL RESERVOIR WITH INTERNAL HEAT TRANSFER INTENSIFIERS.**

The weight of empty tank	5,7 kg
Weight of metal hydride	7,94 kg
Total weight of filled tank with MH	13,64 kg
Volume of metal hydride	0,0028 m <sup>3</sup>
Stored hydrogen mass	0,105 kg
Hydrogen volume	1,25 m <sup>3</sup>
Generated heat in tank	12500 kJ

### III. SIMULATION OF THE HEAT TRANSFER OF THE DESIGNED TANK OF ATYPICAL SHAPE WITH AN INTERNAL HEAT TRANSFER INTENSIFIER

In the following section, the problem of heat transfer in the designed atypical tank is solved, where heat is generated through hydrogen refueling into the structure of the metal alloy. This generated heat must be dissipated and cooled to increase the kinetics of hydrogen absorption and, in addition, to store a larger amount of hydrogen in the structure of the metal alloy. The way in which it would be possible to cool the tank is, for example, to immerse the entire tank in the cooling liquid, which would, however, only cool the perimeter of the tank. The result of this simulation is shown in FIG 3.

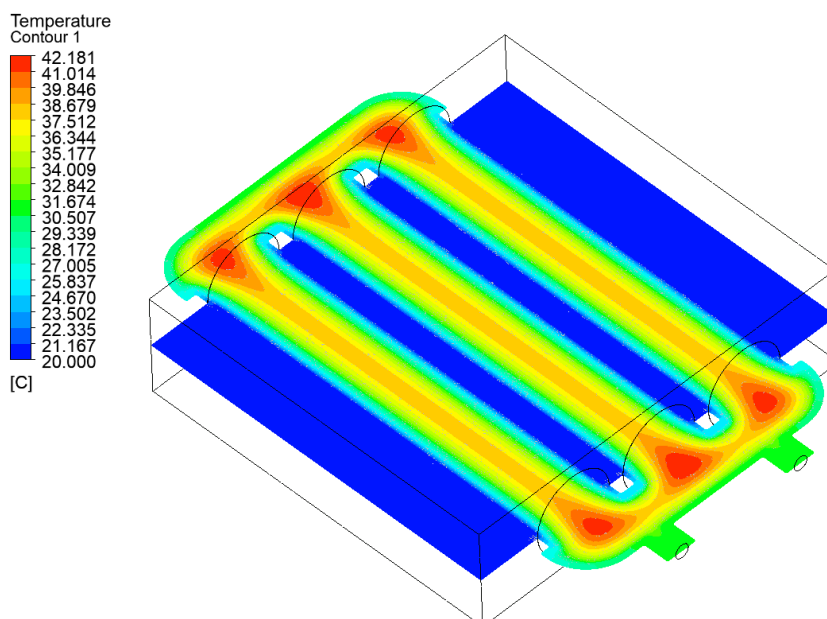


**FIGURE 3: Generated temperature fields for an atypical reservoir immersed in a coolant.**

To effectively remove the heat from the tanks core, it is possible to use a passive heat exchanger or an internal heat transfer intensifier, which will be in cylindrical seamless pipes. The intensifier serves as a passive cooling element, which means that the heat generated in the core of the tank is dissipated outwards in the direction of the ribs to the inner wall of the cylindrical seamless pipes, where this heat is then effectively cooled by the cooling liquid.

### 3.1 Setting up the heat transfer simulation of the storage tank with an internal intensifier

In this simulation, the temperature fields that arise on the entire volume of the atypical metal hydride reservoir will be investigated, and the temperature fields in the section of the cylindrical parts, where the internal heat transfer intensifier is located, will also be investigated. The process of hydrogen absorption into the structure of the metal alloy normally takes about 20 minutes when using an alloy based on LaCeNi, which also represents the total simulation time. Before starting the simulation, it is necessary to create a simulation model and generate a mesh of finite elements. Generated mesh represents approximately 7,000,000 nodes and 1,500,000 volumetric finite elements.

Another part of the simulation setup is defining the boundary conditions. The first step is to define the domains that define the overall simulation model. Specified domains include steel tank, metal hydride alloy, heat transfer intensifiers, and coolant. It is further necessary to define the initialization conditions for each domain, i.e., the initialization temperature is set to the ambient laboratory temperature, which is 20°C. In the domain of the cooling liquid, it is necessary to define the inlet and outlet of coolant, and in the domain of the metal hydride, it is necessary to define the heat generation power during the hydrogen absorption process. The power value is set to  $107 \cdot 10^3 \text{ W} \cdot \text{m}^{-3}$ .

Another thing that needs to be done before starting the simulation is to define the material properties and individual connections between the defined domains. FIG 4 shows the prepared simulation model.

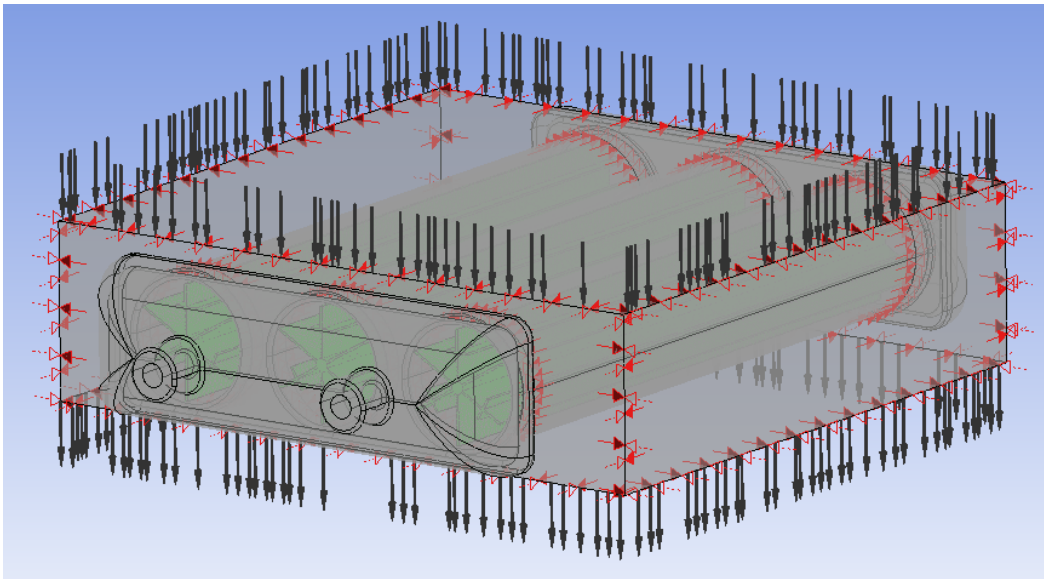


**FIGURE 4: Finite element mesh of the first simulation**

#### 3.1.1 Simulation results

The maximum temperatures that occurred in the tank were mainly in bottoms, where they reached a temperature of 42.1°C. However, the average temperature in the cylindrical parts of the tank, in which the heat transfer intensifiers were located inside, was approximately 28°C. This means that the kinetics of absorption as well as the amount of stored hydrogen will be higher than if the internal intensifier was not inserted. According to the PCI curve of the selected metal hydride alloy LaCeNi at the obtained temperature, the mass ratio reaches 1.8% wt.

By optimizing the geometrical shape of the internal heat exchanger, it is possible to reduce the maximum temperatures even more.

The result of the simulation of the temperature fields on the entire volume of the reservoir can be seen in FIG 5, and the result of the simulation of the temperature fields in the section of cylindrical seamless pipes with a heat transfer intensifier can be seen in FIG 6.

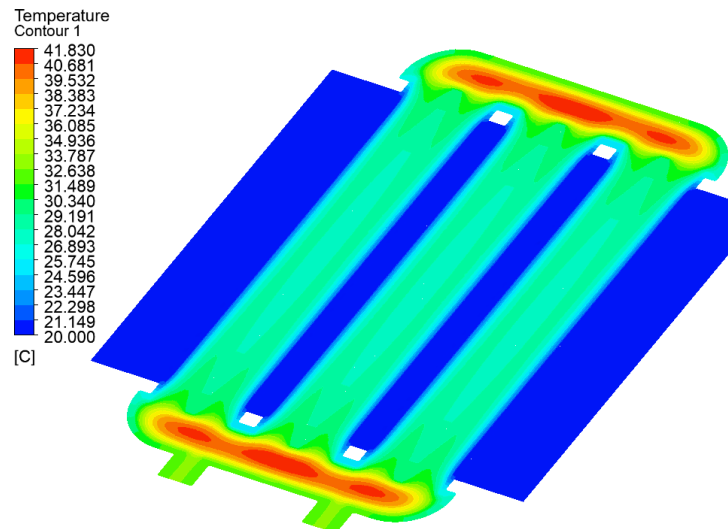


**FIGURE 5: Generated temperature fields in an atypical metal hydride tank with heat intensifiers**

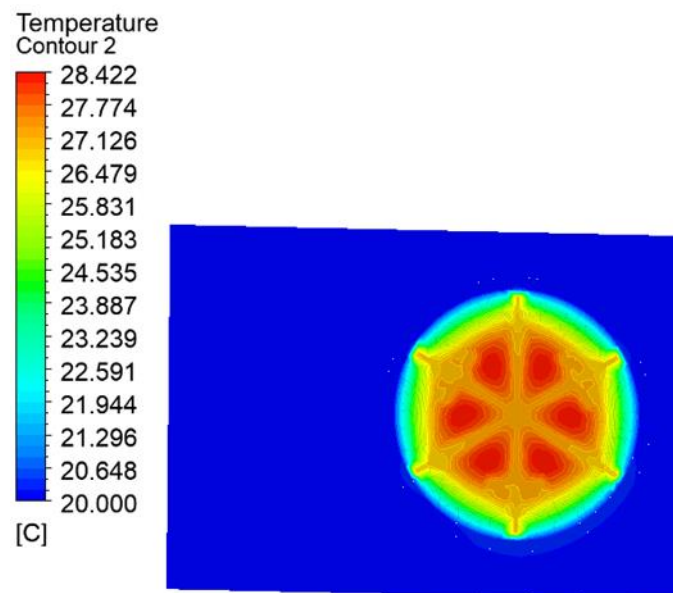


**FIGURE 6: Generated temperature fields in the section of the cylindrical wall of a seamless pipe**

#### IV. CONCLUSION

In the Part 1 article, the temperature fields where cooling of the designed atypical metal hydride tank was not considered were investigated to find the maximum generated temperatures that reached about 50°C. Subsequently, the investigated tank was immersed in the cooling liquid, which reduced the maximum temperature to approximately 41.5°C.

The aim of this article was to create an effective system for dissipating the generated heat from the core of the storage tank through a suitable passive cooler, i.e. an internal heat transfer intensifier, so that the maximum temperature of the designed storage tank could be reduced even more.

After the application of the internal heat transfer intensifier, the maximum temperature in the cylindrical parts was reduced to a temperature of 28.4°C, which significantly increases the kinetics of hydrogen absorption into the metal alloy structure. By properly optimizing the shape of the intensifier, it would be possible to reduce the temperature even more, which will be another part of the research.

### ACKNOWLEDGEMENTS

This paper was written with financial support from the VEGA granting agency within the projects no. 1/0224/23 and no. 1/0532/22, from the KEGA granting agency within the project no. 012TUKE-4/2022 and with financial support from the APVV granting agency within the projects no. APVV-15-0202, no. APVV-20-0205 and no. APVV-21-0274.

### REFERENCES

- [1] Afzal, M. Mane, R. Sharma, P.: Heat transfer techniques in metal hydride hydrogen storage: A review. *International Journal of Hydrogen Energy* 42, 2017.
- [2] Lipman, E. T., Weber, Z. A. *Fuel Cells and Hydrogen Production*. New York: Springer Science+Business Media, 2018. ISBN 978-1-4939-7789-5.
- [3] Stolten, D. (2010). *Hydrogen and Fuel Cells*, Weinheim: Wiley, 2010, 908 p. ISBN 978-3-527-32711-9.
- [4] Brestovič, T., Jasmínská, N. *Numerické metódy a modelovanie v energetike*, Košice, SJF TU v Košiciach, 2015. ISBN 978-80-553-0223-2.
- [5] Murín, Justín; Hrabovský, Juraj; Kutiš, Vladimír. *Metóda Konečných Prvkov Vybrané kapitoly pre mechatronikov*, Slovenská technická univerzita v Bratislave, 2014.
- [6] Ravinger, Ján. *Numerical methods in theory of structures*, Slovenská technická univerzita v Bratislave 2014.
- [7] Sankir, M a Sankir, D, N.: *Hydrogen Storage Technologies*. Scrivener Publishing LLC, 2018. ISBN 978-1-119-45988-0.
- [8] STN EN 13322-2, *Prepravné fľaše na plyny. Navrhovanie a výroba znovuplniteľných oceľových fliaš na plyny. Časť 2: Nehrdzavejúce ocele*, 2003.
- [9] Valizadeh, M. Delavar, A, M. Farhadi, M.: Numerical simulation of heat and mass transfer during hydrogen desorption in metal hydride storage tank by Lattice Boltzmann method. *International Journal of Hydrogen Energy* 41, 2016.

# Design of a Model of Liquid Feeder to an Incinerator of Hazardous Waste and its Optimization from the Cooling Point of View: Part II

Ivan Mihálik<sup>1\*</sup>, Marián Lázár<sup>2</sup>, Tomáš Brestovič<sup>3</sup>, Peter Milenovský<sup>4</sup>

Department of Energy Engineering, Faculty of Mechanical Engineering, Technical University of Košice,  
Vysokoškolská 4, 042 00 Košice, Slovakia

\*Corresponding Author

Received: 03 November 2023/ Revised: 15 November 2023/ Accepted: 21 November 2023/ Published: 30-11-2023

Copyright © 2023 International Journal of Engineering Research and Science

This is an Open-Access article distributed under the terms of the Creative Commons Attribution Non-Commercial License (<https://creativecommons.org/licenses/by-nc/4.0>) which permits unrestricted Non-commercial use, distribution, and reproduction in any medium, provided the original work is properly cited.

**Abstract**— A series of articles aimed at the cooling of the liquid radioactive waste feeder into the incinerator space optimization. The second part examines ion-exchange resins used in the nuclear industry and the possibilities of their combustion. A 3D model of a radioactive waste feeder with different variants of cooling pipes is proposed. Using numerical simulation, the cooling efficiency of individual variants is compared.

**Keywords**— *Radioactive Waste, Ion-Exchange Resin, CFD Simulation, Heat Transfer, Cooling Optimization.*

## I. INTRODUCTION

The first part of the article discussed individual types of radioactive waste and the possibility of their incineration. However, ion-exchange resins (IONEX) are also used in various nuclear power plant systems for the purpose of removing specific contaminants. For example, Amberlite IRN78 with a maximum operating temperature of 60 °C is used to remove traces of chlorine contamination from the reactor cooling system and to control the boron level in the primary system of the power plant. It is also used for exhaust cleaning of the steam generator. Due to its high stability and purity, Amberlite IRN150 with a maximum operating temperature of 60 °C can also be used for cleaning the cooling water of the primary circuit. Amberlite IRN97 H with a maximum operating temperature of 120 °C is used to regulate the pH of the reactor coolant, to remove fission products and to remove Caesium-137 from water vapor.

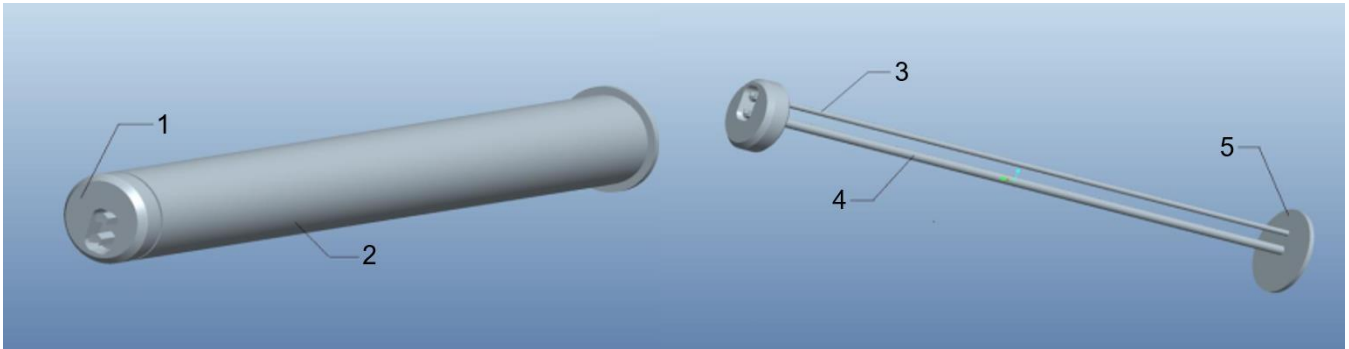
The main function of IONEXes is the ability to bind ions contained in the liquid on their surface, which are subsequently exchanged for positively charged ions. They therefore serve as a medium for ion exchange. These are usually small porous balls with a diameter in the range of 0.3 – 1.2 mm. The porous surface provides a larger area for ion exchange. According to the size of the pores, IONEXes are divided into macroporous and gel. Gel IONEXes have a smaller pore size and are mechanically less resistant.

There are natural or synthetic IONEXes of organic or inorganic origin. Since the IONEXes used in nuclear power plants are mostly of organic origin, burning them in a dry state is not problematic. Combustion of IONEXes in a dry state is possible through fluidic combustion devices with problem-free transport of IONEXes in the form of pellets and at the same time with good air access, which is essential for high efficiency combustion. Feeding IONEXes with a high water content of approximately 40% into the furnace is problematic due to the formation of large clumps and very rapid settling of particles in a liquid transport medium. A suitable medium capable of transporting these particles is, for example, foam (liquid - gas) with sufficient thermal and temporal stability. The advantage is undemanding production directly at the place of consumption with acceptable energy requirements. Among the disadvantages is the negative impact of water on the energy balance of combustion.

## II. FEEDER MODEL AND ITS COOLING PIPE VARIANTS

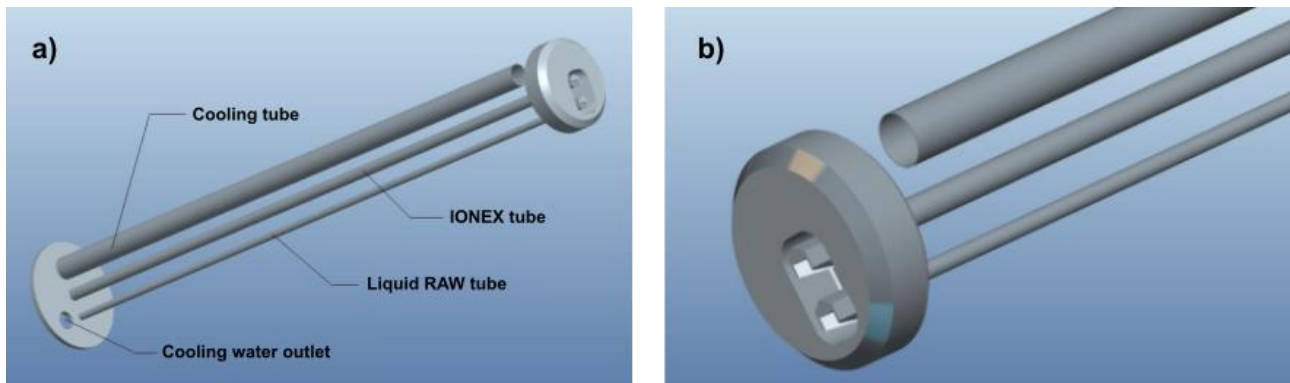
Figure 1 shows the basic model of the radioactive waste feeder without the cooling pipe. On the left, the feeder is shown as seen from the outside, on the right is a view of the inside of the feeder without the outer casing. The outer shell located between the face and the flange has a diameter of 202 mm. The diameter of the pipe intended for IONEXes feeding is 24 mm.

The diameter of the pipe used for the supply of liquid radioactive waste (RAW) is 16 mm. The length of both pipes is 1,500 mm.



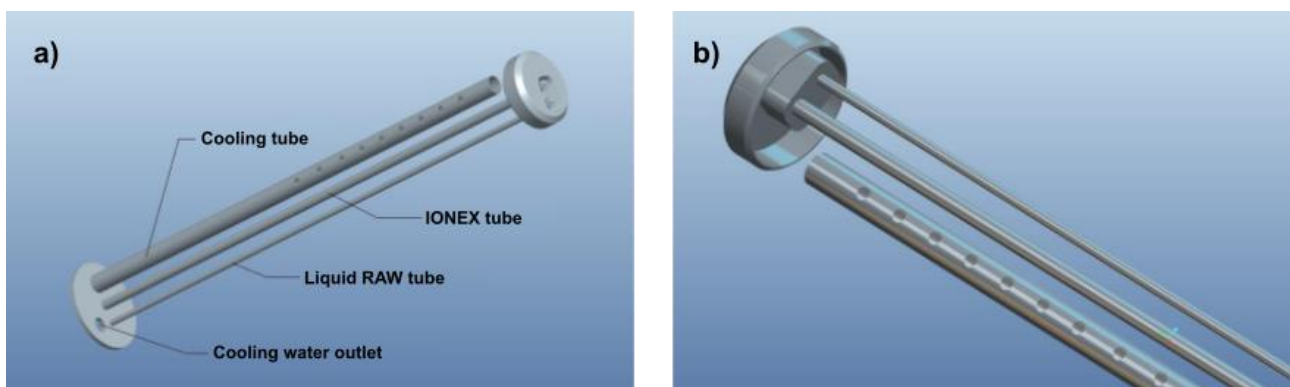
**FIGURE 1: 3D model of the feeder without the cooling pipe: 1 – Front with nozzles; 2 – Outer shell; 3 – Pipe for the supply of a mixture of oil and liquid RAW; 4 – Pipe for the supply of a foam and IONEXes; 5 – Flange.**

Figure 2 shows variant no. 1 of the cooling pipe. It is a reference model and at the same time the simplest design solution. The length of the cooling tube is 1400 mm, while its open end is located at a distance of 100 mm from the face of the feeder. The diameter of the cooling pipe is 50 mm. The diameter of the opening for the cooling water outlet is 40 mm.



**FIGURE 2: a) Variant no. 1. b) Detail of the end of the cooling pipe variant no. 1.**

The cooling tube of variant no. 2 (Figure 3) has the same shape, length and diameter compared to variant no. 1. The difference lies in the creation of 9 holes with a diameter of 20 mm. The distance of the first hole from the open end of the cooling tube is 102 mm. The distance between individual holes is 70 mm. According to the assumption, the creation of holes in the cooling tube should result in the formation of a water vortex and thus the overall improvement of the cooling of the feeder shell.



**FIGURE 3: a) Variant no. 2. b) Detail of the cooling pipe variant no. 2.**

The bent end of the cooling tube of variant no. 3 at an angle of  $45^\circ$  (Figure 4) supports the creation of a circular flow of cooling liquid at the head of the feeder. The cooling liquid should reach higher speeds in that place, which prevents excessive

overheating of the liquid above the permitted temperature. This variant does not contain any holes. The diameter and length of the cooling tube is the same as for variant no. 1.

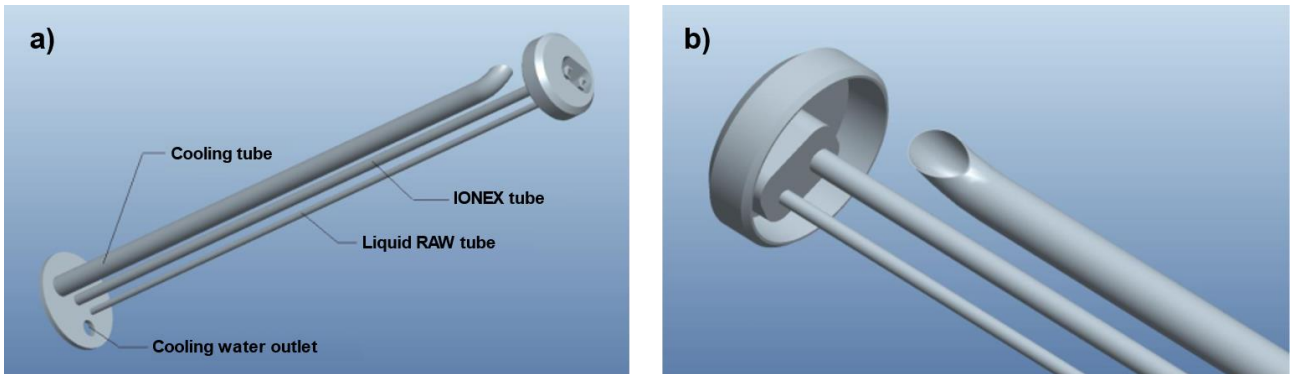


**FIGURE 4: a) Variant no. 3. b) Detail of the end of the cooling pipe variant no. 3.**

**III. MESH GENERATION AND DEFINING SIMULATION CONDITIONS**

The Tetrahedron type mesh with an element size of  $5 \cdot 10^{-4}$  m is dense enough due to the dimensions of the model (Figure 5a) to provide accurate simulation results with acceptable hardware requirements. However, in order to obtain sufficiently accurate results, an additional densification of the mesh is necessary in the area of boundary layers at the boundaries of environments with different properties. In the case of the feeder model, there are 3 boundary layers. The calculation of the distance of the boundary layer from the wall was carried out in the program y+, while the distance from the wall of the shell, from the wall of the cooling tube and from the face of the feeder was determined. The individual parameters required for the calculation of the boundary layer and the subsequent resulting distances of the boundary layers are listed in Table 1.

**TABLE 1**

**PARAMETERS FOR THE CALCULATION OF BOUNDARY LAYERS AND THE RESULTING DISTANCES OF BOUNDARY LAYERS**

	Mantle boundary layer	Cooling tube boundary layer	Feeder face boundary layer
Fluid velocity ( $m \cdot s^{-1}$ )	2.12	0.397	2.12
Length of the boundary layer (m)	1.56	1.43	0.101
Dimensionless distance	1		
Density ( $kg \cdot m^{-3}$ )	0.4625		
Dynamic viscosity ( $Pa \cdot s$ )	$34.29172 \cdot 10^{-6}$		
Distance from the wall (mm)	0.5912	2.5236	0.4085

As part of setting the environment properties, the cooling water inlet and outlet are defined in Figure 5b.

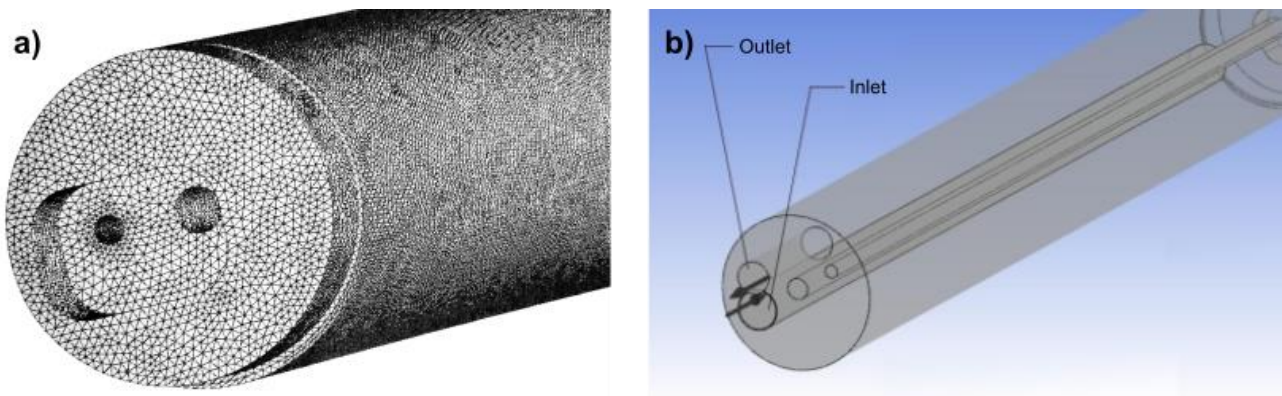


**FIGURE 5: a) Mesh of the feeder model. b) Defining the coolant inlet and outlet.**

Due to the changing properties and parameters of water when the temperature changes, it is not suitable for simulation purposes to use table values. More accurate simulation results can be obtained by defining water properties through equations (1-4) obtained by regression analysis based on table values:

$$\rho = 1000 - 6.714 \cdot 10^{-2} \cdot t - 3.571 \cdot 10^{-3} \cdot t^2 \tag{1}$$

where  $\rho$  is density of water ( $\text{kg}\cdot\text{m}^{-3}$ ) and  $t$  is temperature of water ( $^{\circ}\text{C}$ ).

$$\eta = 2.596 \cdot 10^{-4} + 11.046 \cdot 10^6 \cdot e^{-2\left(\frac{t+1331}{395}\right)^2} \tag{2}$$

where  $\eta$  is dynamic viscosity of water ( $\text{Pa}\cdot\text{s}$ ).

$$c_p = 4220.2 - 3.38 \cdot t + 9.111 \cdot 10^{-2} \cdot t^2 - 9.4213 \cdot 10^{-4} \cdot t^3 + 3.646 \cdot 10^{-6} \cdot t^4 \tag{3}$$

where  $c_p$  is isobaric specific heat capacity of water ( $\text{J}\cdot\text{kg}^{-1}\cdot\text{K}^{-1}$ )

$$\lambda = 0.5565 + 2.112 \cdot 10^{-3} \cdot t - 8.661 \cdot 10^{-6} \cdot t^2 \tag{4}$$

where  $\lambda$  is thermal conductivity coefficient ( $\text{W}\cdot\text{m}^{-1}\cdot\text{K}^{-1}$ )

#### IV. COMPARISON OF SIMULATION RESULTS

The resulting temperature layouts obtained through numerical simulation for individual variants of the feeder are shown in Figures 6 to 8. Variant no. 1 shown in Figure 6 is suitable in terms of the maximum permitted temperature of  $60^{\circ}\text{C}$ , as the maximum temperature reached in this case is  $59.2^{\circ}\text{C}$ . In addition, this temperature is not reached in the pipe area, but it is a surface temperature on the casing of the feeder, which does not have a direct effect on the operation of the device.

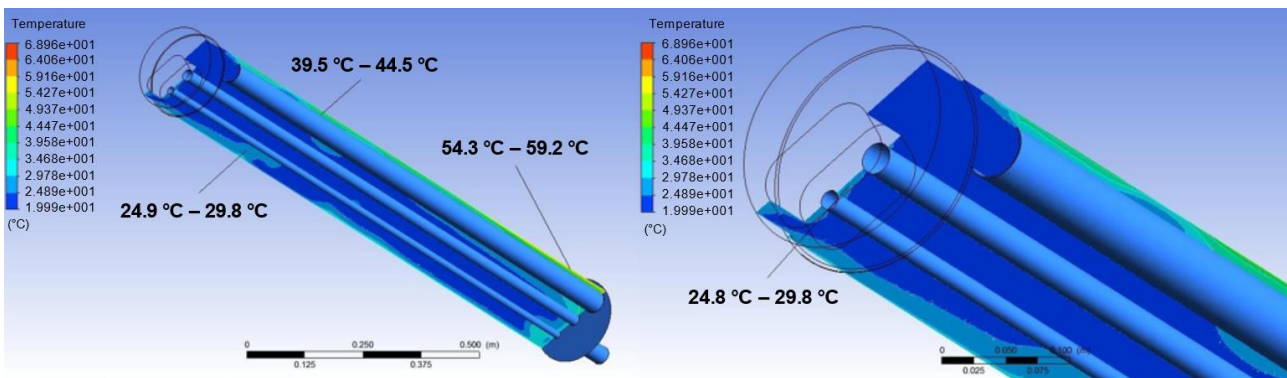


FIGURE 6: Temperature field – Variant no. 1.

Variant no. 2 in Figure 7 is also within the permitted temperature range. The maximum temperature of  $54.2^{\circ}\text{C}$  is a little lower than in the previous variant, which is again the temperature of the feeder casing.

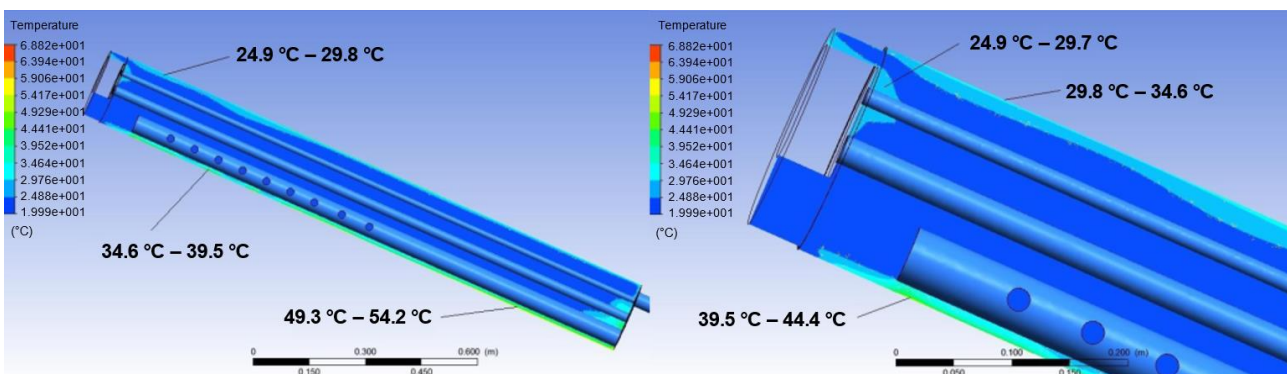
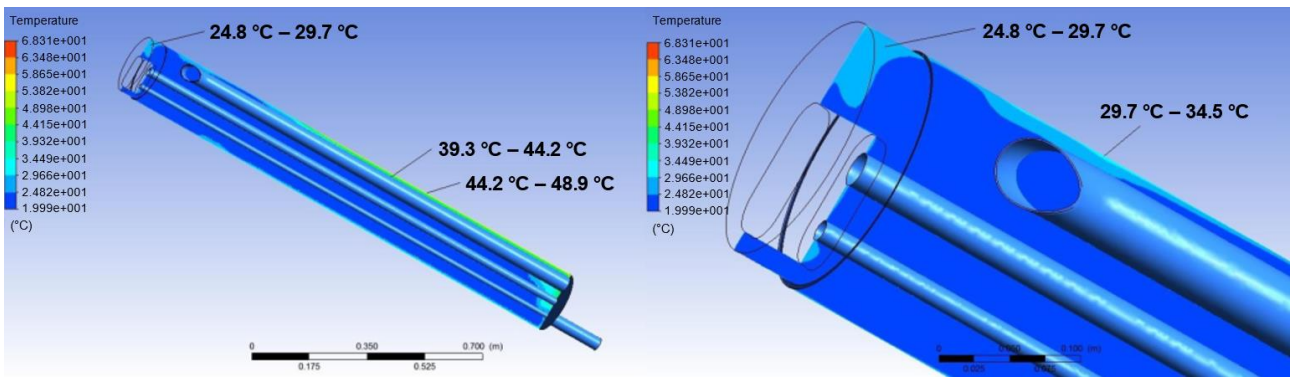


FIGURE 7: Temperature field – Variant no. 2.

The temperature field of variant no. 3 (Figure 8) reaches the lowest maximum value of  $48.9^{\circ}\text{C}$ , so in terms of temperatures it appears to be the most suitable variant.



**FIGURE 8: Temperature field – Variant no. 3.**

The direction and speed of the cooling water flow of the individual variants are compared in Figure 9.

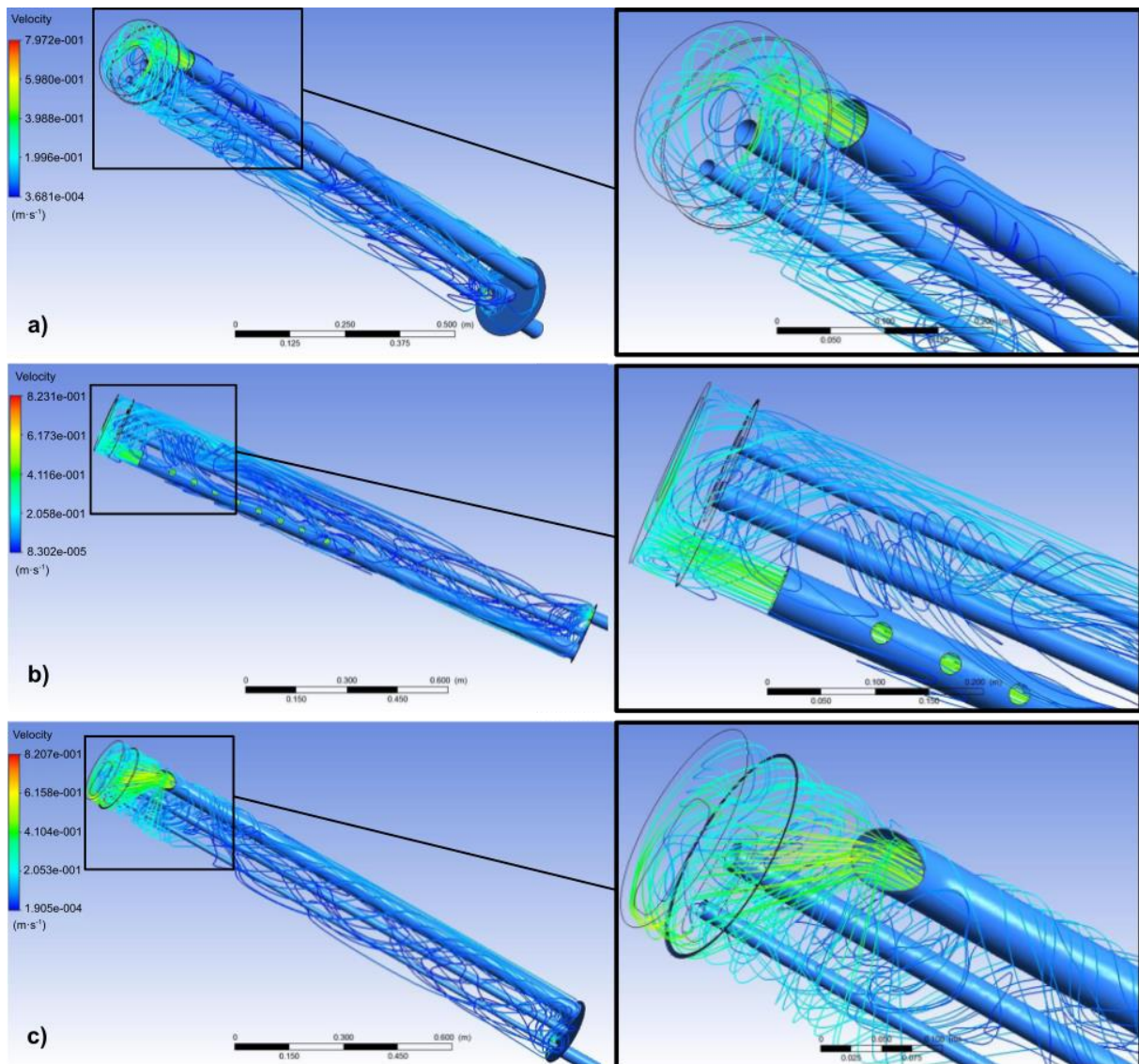


**FIGURE 9: Cooling water flow. a) Variant no. 1. b) Variant no. 2. c) Variant no. 3.**

When comparing variant no. 1 and variant no. 2, it is not possible to observe significant changes in the flow. The holes created in the cooling tube of variant no. 2 do not affect the nature of the flow and do not contribute to the formation of vortices. Therefore, their creation has no justification from a structural and operational point of view. On the contrary, the comparison of variant no. 1 and variant no. 3 with the bent end of the cooling tube shows a more significant change in flow in the area of the feeder face.

## V. CONCLUSION

The production of electricity in nuclear power plants requires a high technical level of many devices for safe and continuous operation, including the RAW and IONEX feeders to the furnace premises. Considering the environment of the furnace with high temperatures and the limited operating temperatures of individual IONEXes, it is necessary to ensure effective cooling of these devices. When considering the mass flow of water determined by the calculation in Part I at the level of  $Q_m = 0.779 \text{ kg}\cdot\text{s}^{-1}$ , all 3 proposed variants are satisfactory in terms of operating temperature, while the best results in the field of cooling are provided by variant no. 3 with a curved end of the tube with a maximum temperature of 48.9 °C. Further reduction of temperatures in the feeder can be achieved, for example, by increasing the cooling water flow to the level of 1.17 kg·s<sup>-1</sup>. With this increased flow, it would be possible to additionally reduce the maximum temperature by 11 °C.

## ACKNOWLEDGEMENTS

This paper was written with financial support from the VEGA granting agency within the projects no. 1/0224/23 and no. 1/0532/22, from the KEGA granting agency within the project no. 012TUKE-4/2022 and with financial support from the APVV granting agency within the projects no. APVV-15-0202, no. APVV-20-0205 and no. APVV-21-0274.

## REFERENCES

- [1] G. Darmograi, B. PreLOT, A. Geneste, L.-Ch. De Menoryal, J. Zajac, "Removal of three anionic orange-type dyes and Cr(VI) oxyanion from aqueous solutions onto strongly basic anion-exchange resin. The effect of single-component and competitive adsorption". In: *Colloids and Surfaces A: Physicochemical and Engineering Aspects*, 2016. Volume 508, pages 240-250, ISSN 0927-7757. DOI: <<https://doi.org/10.1016/j.colsurfa.2016.08.063>>
- [2] M. Sillanpää, M. Shestakova, "Chapter 3 - Emerging and Combined Electrochemical Methods". In: *Electrochemical Water Treatment Methods*, 2017. Butterworth-Heinemann. Pages 131-225. ISBN 9780128114629. DOI: <<https://doi.org/10.1016/B978-0-12-811462-9.00003-7>>
- [3] Evoqua. "Ion Exchange Resins for Nuclear Power Plants" [online]. Available at: <<https://www.evoqua.com/en/markets/applications/ion-exchange-resins-for-nuclear-power-plants/>> [cit. 10-10-2023]
- [4] J. Irving, "WATER TREATMENT | Overview: Ion Exchange". In: *Encyclopedia of Separation Science*. Academic Press, 2000. Pages 4469-4477, ISBN 9780122267703. DOI: <<https://doi.org/10.1016/B0-12-226770-2/02031-7>>
- [5] S. Lecheler, "Computational Fluid Dynamics: Getting Started Quickly With ANSYS CFX 18 Through Simple Examples". 2022. Springer, 1st edition. 220 pages. ISBN 978-3658384524.
- [6] T. Brestovič, N. Jasminská, "Numerické metódy a modelovanie v energetike", 2015. Strojnícka fakulta Technickej univerzity v Košiciach. 113 pages. ISBN 978-80-553-2067-0.

# Liquid Impact Sheet Metal Deformation of Superni (Inconel) 718 using Inclined Edge (Conical) DIE

E. Hazya<sup>1</sup>, Dr S Gajanana<sup>2</sup>, Dr. P. Laxminarayana<sup>3</sup>

<sup>1</sup>Assistant Professor, Mechanical Engineering Department, College of Engineering, JNTUH. Hyderabad, India

<sup>2</sup>Professor, Mechanical Engineering Department, M.V.S.R. Engineering College, Hyderabad, India

<sup>3</sup>Professor, Mechanical Engineering Department, College of Engineering, Osmania University, Hyderabad, India

\*Corresponding Author

Received: 04 November 2023/ Revised: 16 November 2023/ Accepted: 21 November 2023/ Published: 30-11-2023

Copyright © 2023 International Journal of Engineering Research and Science

This is an Open-Access article distributed under the terms of the Creative Commons Attribution

Non-Commercial License (<https://creativecommons.org/licenses/by-nc/4.0>) which permits unrestricted

Non-commercial use, distribution, and reproduction in any medium, provided the original work is properly cited.

**Abstract**— Liquid/Hydraulic impact forming is a sheet metal forming process in which a dead weight drop freely from a certain height over a piston working inside a cylinder containing liquid or hydraulic fluid, generates shock waves which reach the sheet metal kept at a lower part of the cylinder and deforms it to the shape of the die placed below the sheet metal. In the present work Taguchi design of experiments (DoE) technique is used in order to find the effect of input parameters on impact force for deformation of superni (Inconel) 718 using inclined edge die. Contribution of each factor on output is determined by ANOVA (Analysis of Variance) and also an attempt is made towards green manufacturing by adopting used gear and vegetable oils as operating fluids. The outcome of this research will be very much useful for medium and small segment industries in getting the pre-form of the product with least cost.

**Keywords**— Liquid/Hydraulic Impact Forming, Taguchi Design of Experiments (DoE), Inconel 718, Green Manufacturing, Analysis of Variance (ANOVA), Hydraulic Fluid

## I. INTRODUCTION

### 1.1 Liquid impact forming:

Oil can be considered as a homogeneous fluid incapable of supporting any shear. An impulsive load causes a rearrangement of fluid by flow through any boundary displacements caused by loading. A change in the pressure results in change in volume and a spontaneous local pressure is transmitted to other stations in the fluid through “elastic wave of disturbance” commonly called as stress waves. The stress waves are longitudinal waves and travel at the speed of sound of the particular fluid. The velocity of the stress waves is given by:

$$C = \sqrt{k / \rho}$$

Where  $k$  = bulk modulus of the fluid,  $\rho$  = density of the fluid

The pressure profile of a liquid hammer pulse can be calculated from the Joukowsky equation:

$$\frac{\delta P}{\delta t} = \rho a \frac{\delta \vartheta}{\delta t}$$

So for a valve closing instantaneously, the maximum magnitude of the Hydraulic liquid hammer pulse is given by:

$$\Delta P = \rho a \Delta \vartheta$$

Where  $\Delta P$  is the magnitude of the pressure wave (Pa),  $\rho$  is the density of the fluid ( $\text{kgm}^{-3}$ ), ‘ $a$ ’ is the speed of sound in the fluid ( $\text{ms}^{-1}$ ), and  $\Delta \vartheta$  is the change in the fluid's velocity ( $\text{ms}^{-1}$ ). The pulse is due to Newton’s laws of motion and the continuity equation as applied to the deceleration of a fluid element.

### 1.2 Superni Inconel) 718

Materials with distinctive metallurgical properties – such as an alloy of titanium, nickel, tool steel and other super alloys are primarily used for a specialized application requiring heat and corrosion resistance. These materials exhibit several key

characteristics such as excellent mechanical strength, resistance to creep at high temperature, high work hardening, and corrosion resistance and thus they are the first choice of aerospace, submarine, gas turbine and nuclear industries. However, these properties are generally associated with poor machinability. Hence, machining of such difficult-to-cut materials is quite crucial for the manufacturing sector. Inconel 718 is a Ni-Cr based superalloy and has been widely used in aviation, submarine, nuclear, gas turbine, petroleum industries because of its excellent mechanical properties such as high strength, strong creep resistance, superior wear resistance, resistance to chemical degradation and low thermal conductivity. However, the machining of Inconel 718 using conventional machining process like turning, grinding, broaching or milling is very difficult because of its work-hardening nature, retention of high tensile strength at elevated temperature and low thermal conductivity. The chemical composition of Superni 718 (sheet metal) which is procured for research work from Misha Dhatu Nigam Ltd., (MIDHANI) is as given in table 1. The Ni-based superalloy contains major constituent elements such as Nickel (Ni), Iron (Fe), Chromium (Cr), Molybdenum (Mo), and Cobalt (Co) with some minor elements like Aluminum (Al), Titanium (Ti), and so on. These alloying elements enhance the mechanical characteristics. Where, Ni stabilizes alloy structure and properties at elevated temperatures. Co, Mo, and W increase strength at elevated temperature, Cr, Al, Si enhances oxidation resistance and elevated temperature corrosion resistance, and Carbon (C) increases creep strength. In the present work used oils are used as working liquid for deformation of sheet metal as an approach towards green and sustainable manufacturing. Green manufacturing aims to establish a system which integrates product and process issues. Used lubricating oils, used vegetable oil based coolants, represent a serious problem for environment and human health due to the presence of highly harmful contaminants, being mandatory an adequate management based on efficient collection systems and treatment processes. In this current research work an attempt is made to use these used oils as working fluid in Hydraulic hammer forming to get the forming of Superni/Inconel 718 sheet metal.

**TABLE 1**  
**CHEMICAL COMPOSITION OF SUPERNI (INCONEL) 718**

Element	C	Mn	Si	S	P	Cr	Ni	Mo
Wt%	0.08 Max	0.35 Max	0.35 Max	0.015 Max	0.015 Max	17.0 - 21.0	50.0 – 55.0	2.80 – 3.30
Element	Co	Nb	Ti	Al	B	Cu	Ta	Fe
Wt%	1.0 Max	4.75 – 5.50	0.65 - 1.15	0.2 – 0.8	0.006 Max	0.3 Max	0.05 Max	Bal

## II. OBJECTIVES AND METHODOLOGY

The investigation study is planned with the following objectives:

- Postulation of regression model for Impact force which is considered as output response.
- Adoption of two-level Taguchi design of experiments and selection of test regions for the variables (factors).
- Conducting the experiments as per design matrix.
- Estimation of coefficients of postulated model.
- To perform ANOVA (Analysis of Variance).

A regression model is developed using Minitab to understand the relationship between the input parameters and the target variable resultant impact that is formed due to oil impact forming technique. The process parameters shown in table 2 were taken into consideration and Taguchi Method Orthogonal Array (L8) is adopted to perform the experiment.

Taguchi DoE being most useful in terms of into provided, but don't seem to be usually practical for five or more factors because number of experiments doubles sequentially with addition of every factor. However, if experiments are cheap, easy to perform than go ahead with Taguchi design of experiments. Within the study, Taguchi design of experiments for designing the experiments has been used. The Taguchi method recommends orthogonal arrays for laying out the experiment. For design the experiment firstly select the foremost suitable orthogonal arrays (OA) and to allocate the parameters and interaction of interest to the acceptable columns.

**TABLE 2**  
**INPUT PARAMETERS AND LEVELS WITH OUTPUT RESPONSE**

Factors	Units	Designation	Test levels		Output Response (kN)
			Low	High	
Thickness of specimen (t)	mm	t	0.2	0.5	Impact Force
Height of the hammer (h)	cm	h	190	250	
Weight of the hammer (w)	kg	b	15	25	
Viscosity of the Fluids (o)	Poise	o	9.9	11.4	
(o1: Viscosity of used gear oil, o2 : Viscosity of used vegetable oil)					

### III. EXPERIMENTATION & REGRESSION MODEL DEVELOPMENT

The equipment is arranged on rectangular concrete base wooden block is placed over the concrete base so as to absorb the shock load without damaging the system die holder is kept on the wooden block. Suitable die is selected and placed in the die holder over which the sheet metal (work piece) is located in the shallow counter sunk bore, of the same diameter as the specimen, on the die face. Venting is provided both in the die and die holder, to prevent spring back of the specimen due to compressing of trapped air. Now the cylinder with two 'O' rings are fixed in order to prevent leakage of the working fluid. Cylinder flange and guide bush are mounted on the cylinders in such a way that it is fixed with a m-10 Allen screw. Two swing bolts are used to clamp the cylinder flange and hold the cylinder in position. Plunger along with 'O' ring fixed on it, is inserted through the guide bush into the cylinder. The mating faces of plunger and cylinder were grinded for smooth movement. Wall bracket is fixed in the wall to support the guide mechanism. The guide mechanism comprises of a pulley for lifting the weight. The set of three guide wires are provided to guide the falling weight. The weights are fixed on a disc carrying a one end thread inside the disc and other end locked to the rope by means of an eye end. The die holder is placed on the wooden block. The surface of the die should be free from dust, dirt and other foreign materials to provide good forming. The die is placed in the holder. The specimen is located in the shallow counter sunk bore between the die face and the cylinder. The cylinder cavity is filled with Hydraulic liquid up to desired height by removing the necessary Hydraulic liquid tap screws. Cylinder flange along with the guide bush is located by means of bolts. The plunger is inserted into the cylinder with the 'O' rings in position, up to the Hydraulic liquid level. Predetermined weight is raised to the required height manually by means of the rope over the pulley. Then it is released suddenly. The deformation of the work piece takes place by the shock waves in the Hydraulic liquid generated by the impact of the freely falling weights. The swing bolt is unfastened. The wire fixed to the cylinder flange lifts the cylinder along with the plunger, guide and guide bush. The formed specimen is removed from the shallow counter sunk bore and replaced by the new specimen. The cyclic process can be repeated by varying loads, energy input and Hydraulic liquid column heights.

The Taguchi (L8) design matrix of experimentation and output are given in the Table-3

**TABLE 3**  
**TAGUCHI (L8) DESIGN MATRIX WITH RESPONSE**

Trail	Thickness of specimen (t)	Height of the hammer (h)	Weight of the hammer (w)	Viscosity of the Fluids (o)	Impact Force (F)
1	0.2	190	15	9.88	11.2915
2	0.2	190	25	11.36	16.4345
3	0.2	250	15	11.36	12.7062
4	0.2	250	25	9.88	22.3318
5	0.5	190	15	11.36	13.302
6	0.5	190	25	9.88	20.5593
7	0.5	250	15	9.88	15.6123
8	0.5	250	25	11.36	22.0909



**FIGURE 1: Experimental Setup**

The experimental response values are used in Minitab and the regression equation generated is as given below.

$$\text{Impact Force} = -0.81 + 7.33 t + 0.0465 h + 0.7126 w - 0.889 o$$

Analysis of variance is done to find out the percentage contribution of each factor and relative significance of each factor for Impact force the values are tabulated in table 4.

**TABLE 4  
ANALYSIS OF VARIANCE (ANOVA)**

	Source	Contribution
<b>Analysis of variance (ANOVA)</b>	Thickness of specimen (t)	7.25%
	Height of the hammer (h)	11.64%
	Weight of the hammer (w)	76.01%
	Viscosity of the Fluids (o)	2.59%
	Error	2.51%

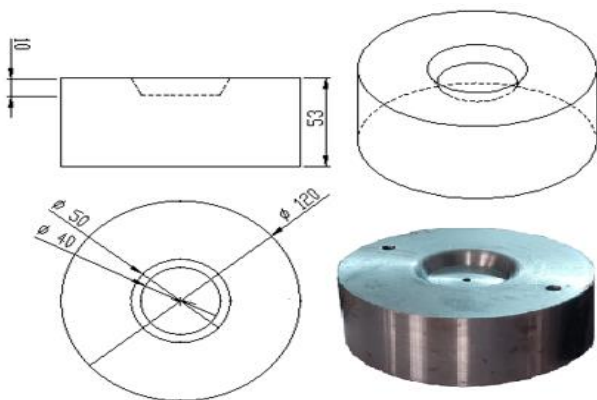


**FIGURE 2: Details of inclined edge die**



**FIGURE 3: Deformed Superni 718work pieces**

**IV. RESULTS AND DISCUSSION**

- Fig.4: Demonstrated that the variation of impact is 7% ie., 28.96 kN to 31.16 kN when the thickness varies from 0.2 mm to 0.5 mm when all the remaining input parameters at low level. When input parameters are at high level the variation of force is less than 7% for change in the thickness of 0.2 mm 0.5 mm. This indicates that loading may be reached the yield phenomenon of material at higher levels of impact parameters.
- Fig.5: Indicates the variation of impact force when the height of hammer changes from 190 cm to 250 cm when input parameters are at low level the variation of force is about 7% whereas for higher level of input parameters it is 7%. This observation n establishes that at higher level of input parameters the force transmitted to the work piece is reducing which may be attributed to dynamics of fluid.
- Fig.6: Shows the variation of impact force when the weight of hammer changed from 15 Kg to 25 Kg. The variation of force when input parameters are at low level is 24% whereas for higher level is 20% this concerned that higher level of parameters considering the yield point phenomenon of work piece material.
- Fig.7: Shows that variation of impact forces when the viscosity changes of fluid from 9.88 to 11.36 Poise. When impact parameters are at low level the impact force is reduced with increase in viscosity by 1.31 kN whereas higher level of input parameters is 1.32 kN. Which may be attributed to the power transmitting ability of fluid in conical die.

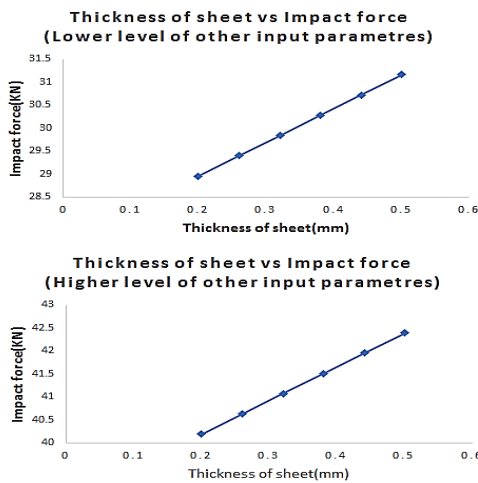


**FIGURE 4: Variation of impact with thickness**

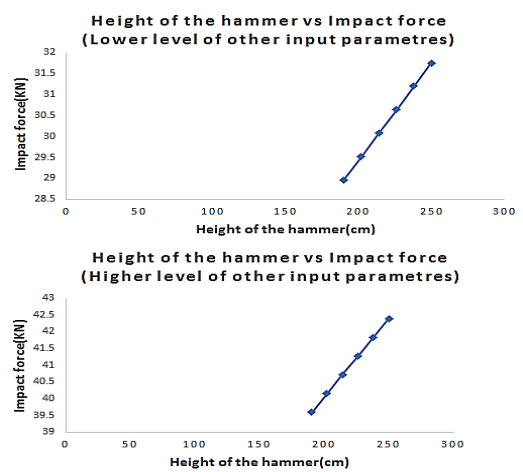


**FIGURE 5: Variation of impact with height of hammer**

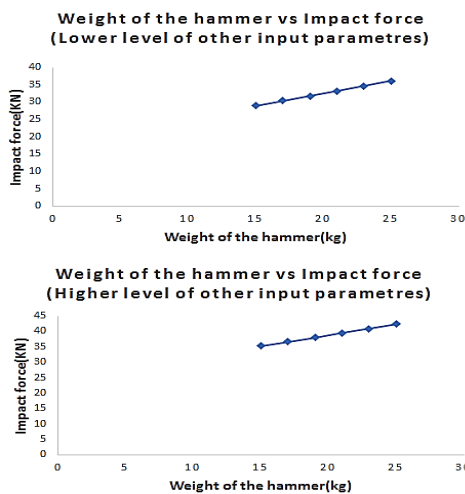


**FIGURE 6: Variation of impact with weight of hammer**

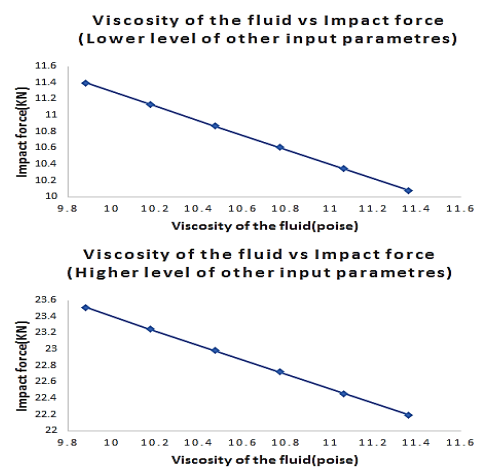


**FIGURE 7: Variation of impact with weight of hammer**

## REFERENCES

- [1] Davis R et al., (1970), "Developments in High Speed Metal Forming", Industrial Press Inc.
- [2] Grieve, et al., (1981), "Some aspects of sheet-metal forming using impact loading through Hydraulic liquid columns", Experimental mechanics, August 1981, 302-308.
- [3] Alder Y.P., et al., (1975) "The Design of Experiments to find Optimal Conditions", MIR publications, Moscow.
- [4] Montgomery D.C.; (1991), "Design and Analysis of Experiments", John Wiley and Sons, New York.
- [5] H.M.T., (1988) "Production technology", TMH, New Delhi.
- [6] P.C. Panday & H.S. Shan "Modern Machining Process".
- [7] Gajanana.S, (2002), "Development of Mathematical Model for Maximum Punch Force" Proceeding of National Conference on Advanced Trends in ME Research and Development, JNTU College of Engineering, Ananthapur, 21<sup>st</sup> Dec, 2002.
- [8] Gajanana.S, (2006), "Optimization of Process Parameters for Hero Honda Exhaust Valve using Design of Experiments" Proceeding of National Conference on Recent Advances in Computer Aided Engineering, Osmania University, Hyderabad, March 3<sup>rd</sup> & 4<sup>th</sup>, 2006.
- [9] M. Barzegar et al (2018), "Analyzing the Drivers of Green Manufacturing Using an Analytic Network Process Method: A Case Study" International Journal of Research in Industrial Engineering, Vol. 7, No. 1 (2018) 61–83.
- [10] Gajanana.S, (2007), "Development Of Mathematical Model For EDM Using Two Factorial Design of Experiments" XXIII National Convention Of Mechanical Engineers And National Seminar On 'Emerging Trends In Manufacturing Systems And Technologies', Hyderabad, September 10-12, 2007.
- [11] Ravinder Kumar, Ashish Kumar Sharma: "Analysis of Hydraulic liquid Hammer Forming on the Sheet Metal", Journal of Information Engineering and Applications, Vol 2, No.1, 2012.
- [12] Xu Jie (2017), "Research on Green Manufacturing Innovation Based on Resource Environment Protection" IOP Conf. Series: Earth and Environmental Science (EEMS 2017).
- [13] Yang Shen, Xiuwu Zhang, "Intelligent manufacturing, green technological innovation and environmental pollution", Journal of Innovation & Knowledge 8 (2023)100384.
- [14] Mohsin Shahzad, Ying Qu, Saif Ur Rehman, Abaid Ullah Zafar, "Adoption of green innovation technology to accelerate sustainable development among manufacturing industry" Journal of Innovation & Knowledge 7 (2022) 100231.
- [15] Navid Rabiee et al, "Green and Sustainable Membranes: A review" Environmental Research 231 (2023) 116133.
- [16] Dr. S. Nallusamy et al, "sustainable green lean manufacturing practices in small scale industries - a case study" International Journal of Applied Engineering Research, ISSN 0973-4562 Vol. 10 No.62 (2015).
- [17] M. Barzegar et al, "Analyzing the Drivers of Green Manufacturing Using an Analytic Network Process Method: A Case Study" International Journal of Research in Industrial Engineering Vol. 7, No. 1 (2018) 61–83.
- [18] Mahakdeep Singh, Kanwarpreet Singh, APS Sethi, "An empirical investigation and prioritizing critical barriers of green manufacturing implementation practices through VIKOR approach" World Journal of Science, Technology and Sustainable Development Vol. 17 No. 2, 2020, pp. 235-254.
- [19] Juan A. Botas et al, Recycling of used lubricating oil: Evaluation of environmental and energy performance by LCA" Resources, Conservation & Recycling, 125 (2017) 315–323.
- [20] Gauri Mahalle, Nitin Kotkunde, Amit Kumar Gupta, and Swadesh Kumar Singh, "Prediction of flow stress behaviour by materials modelling technique for Inconel 718 alloy at elevated temperature" Advances in materials and processing technologies, <https://doi.org/10.1080/2374068X.2020.1728649>
- [21] Gauri Mahalle et al, "Forming and fracture limits of IN718 alloy at elevated temperatures: Experimental and theoretical investigation" Journal of Manufacturing Processes, 56 (2020) 482–499.

# Use of Peltier Cells in the Cooling Process

Romana Dobáková<sup>1</sup>, Lukáš Tóth<sup>2</sup>, Tomáš Brestovič<sup>3</sup>

Department of Energy Engineering, Faculty of Mechanical Engineering, Technical University of Košice, Slovakia

\*Corresponding Author

Received: 04 November 2023/ Revised: 14 November 2023/ Accepted: 20 November 2023/ Published: 30-11-2023

Copyright © 2023 International Journal of Engineering Research and Science

This is an Open-Access article distributed under the terms of the Creative Commons Attribution

Non-Commercial License (<https://creativecommons.org/licenses/by-nc/4.0>) which permits unrestricted

Non-commercial use, distribution, and reproduction in any medium, provided the original work is properly cited.

**Abstract**— Peltier cells represent an interesting alternative to conventional cooling methods and are currently being used in areas where conventional cooling methods are not suitable. They can produce heat and cold when supplied with electricity. The article discusses the possibilities of using Peltier cell technology in the cooling processes of electronic components in an environment where it is not possible to use conventional cooling methods due to their size or the inappropriateness of the given type of cooling. It compares cooling options and describes basic power calculation procedures to cover cooling power needs. Thermoelectric cooling has several advantages, including the absence of a cooling medium, the possibility of precise temperature regulation, small dimensions and a relatively long service life.

**Keywords**— Peltier cells, thermoelectric device, heat transfer.

## I. INTRODUCTION

With the development of science, technology and the use of advanced technologies, new software applications are constantly created with increasing requirements for hardware, and the associated constant increase in computer performance. As power increases, so does the thermal power produced by electronic components, whether in computers or mobile devices, which must be removed from the device to ensure the required power. To prevent the system from malfunctioning, it is necessary to improve the heat dissipation. The need for heat dissipation adjustments arises due to the increasing performance of cooled parts of the computer and other semiconductor components. While in the past only one fan, usually located in the power source, or passive coolers placed on the surface of the most heated elements was sufficient to cool the computer, nowadays most components are supplemented with a cooler and often this cooler is also supplemented with an active part, a fan or water cooling and a heat exchanger, through which the heat accumulated in the coolant is removed to the surroundings.

Radiant heat is generated on the surface of the printed circuit board fitted with semiconductor components and power components, the effects of which on the power components and individual processors of desktop computers and mobile devices affect their proper work. These semiconductor power components produce radiant heat during their operation, so we can consider them as heat sources. Effective cooling makes it possible to use the maximum power of the transistor, processor and thus also the performance of the given components. Performance growth also results in an increase in processor temperature ratios and the related need for better heat dissipation. In addition to the standard method of cooling processors, which is soon a thing of the past, new cooling methods with new cooling elements and technologies are coming to the fore. The use of the Peltier cell in the field of computer technology and primarily mobile technology brings the advantage of the compactness of the cooling device, but at the cost of additional energy consumption compared to passive heat removal systems. The most interesting nowadays is the use of small Peltier cells in the cooling of powerful mobile devices, where there is no possibility of water cooling and air cooling is not a sufficiently efficient way of cooling due to the poor transfer of heat from the core of the device through the plastic protective covers. In such a case, direct contact of the cold side of the Peltier cell provides a better cooling method, while only a passive heat exchanger or a small fan is sufficient to cool the heated side.

## II. THE PRINCIPLE OF THE PELTIER CELL FUNCTION

A Peltier cell is a thermoelectric device that, when an electric current flows, develops different temperatures on the contact surfaces of two conductors, whereby one surface cools and the other heats up (Peltier phenomenon), or vice versa, when different temperatures are supplied, an electric current is generated (Seebeck phenomenon). Peltier cells are most often

constructed in such a way that a larger number of elements, mostly made of semiconductor materials, are connected in series in terms of electric current flow and in parallel in terms of heat flow.

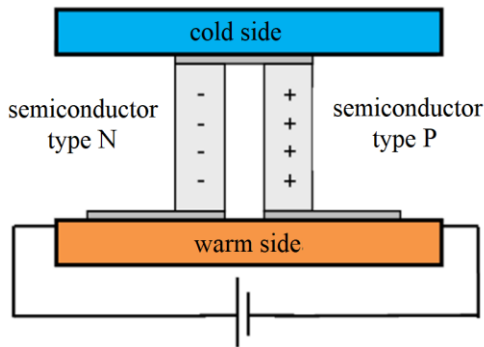


FIGURE 1: One thermoelectric cell

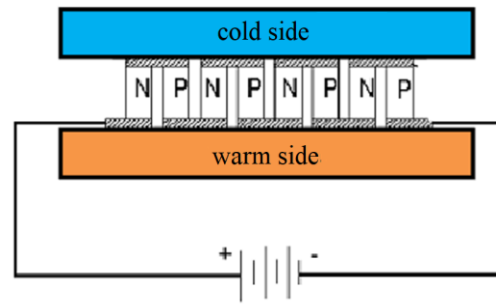


FIGURE 2: Serial connection of thermocouples

Peltier cells consist of several thermocouples connected to a thermoelectric battery. Individual thermocouples are connected using metal bridges that ensure their electrically conductive connection. The mechanical integrity and electrical insulation of the thermocouples are ensured by the ceramic plates on which the thermocouples are fixed. Power supply is provided by two electrodes located on the edges of the cell. Thanks to the process of miniaturization of individual components, including semiconductor parts used in Peltier cells (PC), the thickness of the cell itself and also the weight are reduced, which enables its more comfortable use in the case of mobile applications.

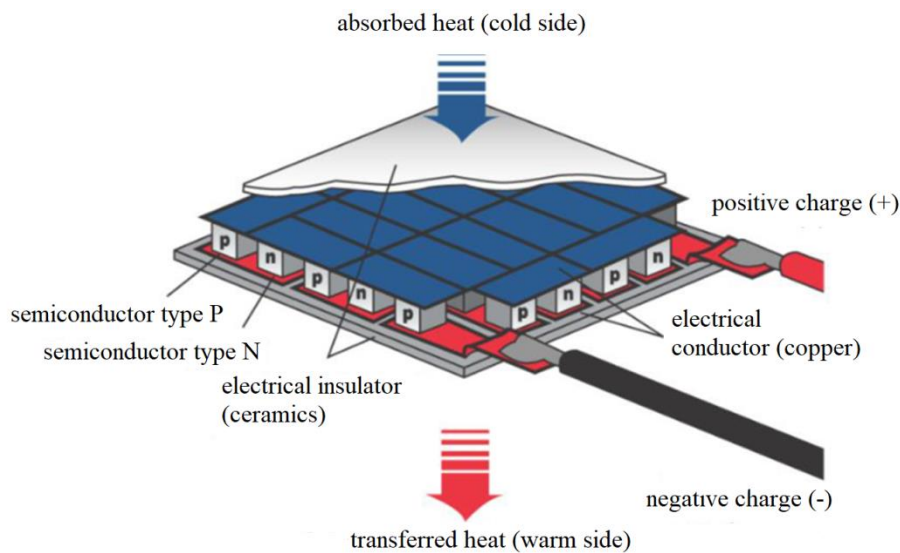


FIGURE 3: Peltier cell

For the heat output entering on the cold side into the Peltier cell PS (fig. 3) this equation applies:

$$P_S = \alpha \cdot I \cdot T_S - \frac{R \cdot I^2}{2} - \lambda \cdot S \cdot \frac{\Delta T}{l} \text{ (W)} \tag{1}$$

where  $\alpha$  is Seebeck's coefficient ( $V \cdot K^{-1}$ ),  $R$  – electrical resistance ( $\Omega$ ),  $I$  – electric current (A),  $T_S$  – temperature on the cold side of PC (K),  $T_H$  – temperature on the warm side of PC (K),  $\lambda$  – the coefficient of thermal conductivity used material ( $W \cdot m^{-1} \cdot K^{-1}$ ),  $S$  – total cross-section of all semiconductor pillars ( $m^2$ ),  $l$  – the height of semiconductor pillars (m),  $\Delta T = T_H - T_S$ .

Thermal power output on the warm side of the PC  $P_H$  can be written in the form:

$$P_H = \alpha \cdot I \cdot T_H + \frac{R \cdot I^2}{2} - \lambda \cdot S \cdot \frac{\Delta T}{l} \text{ (W)} \tag{2}$$

After reaching a steady state, when individual quantities no longer change with time, the law of conservation of energy must apply to the electric power supplied to the cell:

$$P_E = U \cdot I = P_H - P_S = \alpha \cdot I \cdot \Delta T + R \cdot I^2 \quad (\text{W}) \quad (3)$$

The PC cooling efficiency expresses the ratio of the heat removed from the cold side of the cell to the electrical output and can be described by the relation:

$$\eta_{\text{TEC}} = \frac{P_S}{P_E} = \frac{\alpha \cdot I \cdot T_S - \frac{R \cdot I^2}{2} - \lambda \cdot S \cdot \frac{\Delta T}{l}}{\alpha \cdot I \cdot \Delta T + R \cdot I^2} \quad (4)$$

### III. DESIGN OF A COOLING SOLUTION USING PELTIER CELLS

In the experimental cooling design, the used cooling technology and heat removal from the semiconductor component (CPU processor), water in a steel container with a temperature of about 70°C, which was thermally insulated, was used to simulate the supplied heat from the processor. A steel container with a height of 200 mm and a weight of 250.95 g with a diameter of 70 mm was sufficiently insulated with PVC insulation with a thickness of 10 mm and a weight of 36.62 g. The foil served to reduce heat flow by radiation. Sufficient insulation prevents us from transferring energy through thermal conduction, which takes place in solids and liquids. The measurement was based on basic knowledge of the theory of heat and mass transfer.



**FIGURE 4: Insulated steel container**

The choice of PC was based on parameters such as the size of the maximum supply voltage and the size of the maximum current, cell dimensions, the temperature difference between the hot and cold side and, of course, the power of the cell. The cell used is soldered by the manufacturer with BiSn solder, which has a melting temperature of 138°C. For this reason, it is very important not to exceed this temperature during the experiment, otherwise the solder may melt and the cell may be destroyed.

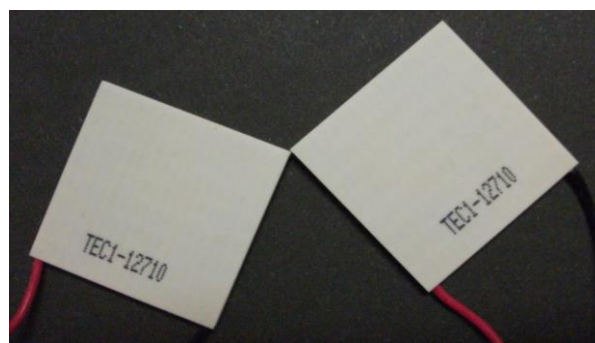


**FIGURE 5: Peltier cell TEC1-12710**

An 80x80mm fan was used for sufficient heat removal from the cooler, with a DC 12V power supply and a power of 2.3W. The Peltier cell was placed with the cold side on the steel cylinder and the warm side on the radiator. Monitoring of temperatures was ensured by the use of 4 pcs of digital temperature sensors of type SMT160-30 in four places with the help of a computer. One sensor measured the temperature on the bottom of the cooler, the other sensor hung freely in the room to monitor the ambient temperature. The third and fourth sensors were placed directly in the steel cylinder, both sensors monitored the temperature of the heated water and its gradual cooling.

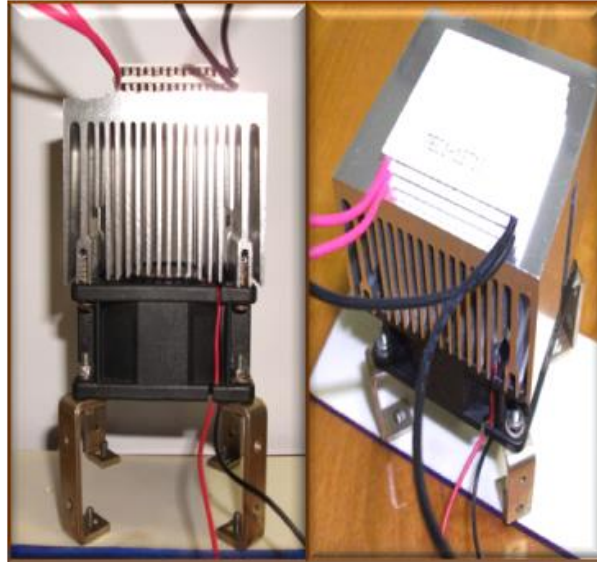


**FIGURE 6: Placement of the Peltier cell**

Uniform cooling of the water in the insulated container was ensured by mixing the water with a motor with an axis at the end of which there was a propeller.



**FIGURE 7: A container with a stirrer**

The measurement was carried out at values other than those specified by the manufacturer of the Peltier cell, namely at a temperature of  $T_H = 60\text{ }^\circ\text{C}$  (temperature of the hot side of the PC - temperature of the cooler) and a current load of 2A, 3A and 6A, which indicated the working behavior of the Peltier cell in the process of cooling semiconductor parts in conditions other than those specified by the manufacturer himself. A very important part of the measurement was monitoring the temperature of the cooler's bottom, which is the temperature of the hot side of the Peltier cell  $T_H = 60\text{ }^\circ\text{C}$ .

**TABLE 1**  
**VALUES OF INDIVIDUAL QUANTITIES DURING EXPERIMENTAL MEASUREMENT**

	current load $I$ (A)	cooler temperature $T_H$ (°C)	volume of water in the cylinder $V_{cylinder}$ (ml)	the initial temperature of the heated water in the cylinder $T_{H2O,cylinder}$ (°C)
Measurement No. 1	2	60	380	70
Measurement No. 2	3	60	380	70
Measurement No. 3	6	60	380	70

The ambient temperature ranged from 21°C to 23°C (desktop computer conditions). The measurement monitors the cooling performance of the Peltier cell under the given cooling conditions with a constant current load of the Peltier cell and a constant temperature of the cooler. The measured values indicate over what time horizon and at what performance of the Peltier cell the gradual cooling of the heated water in the cylinder (or the PC processor) occurs (fig. 8).

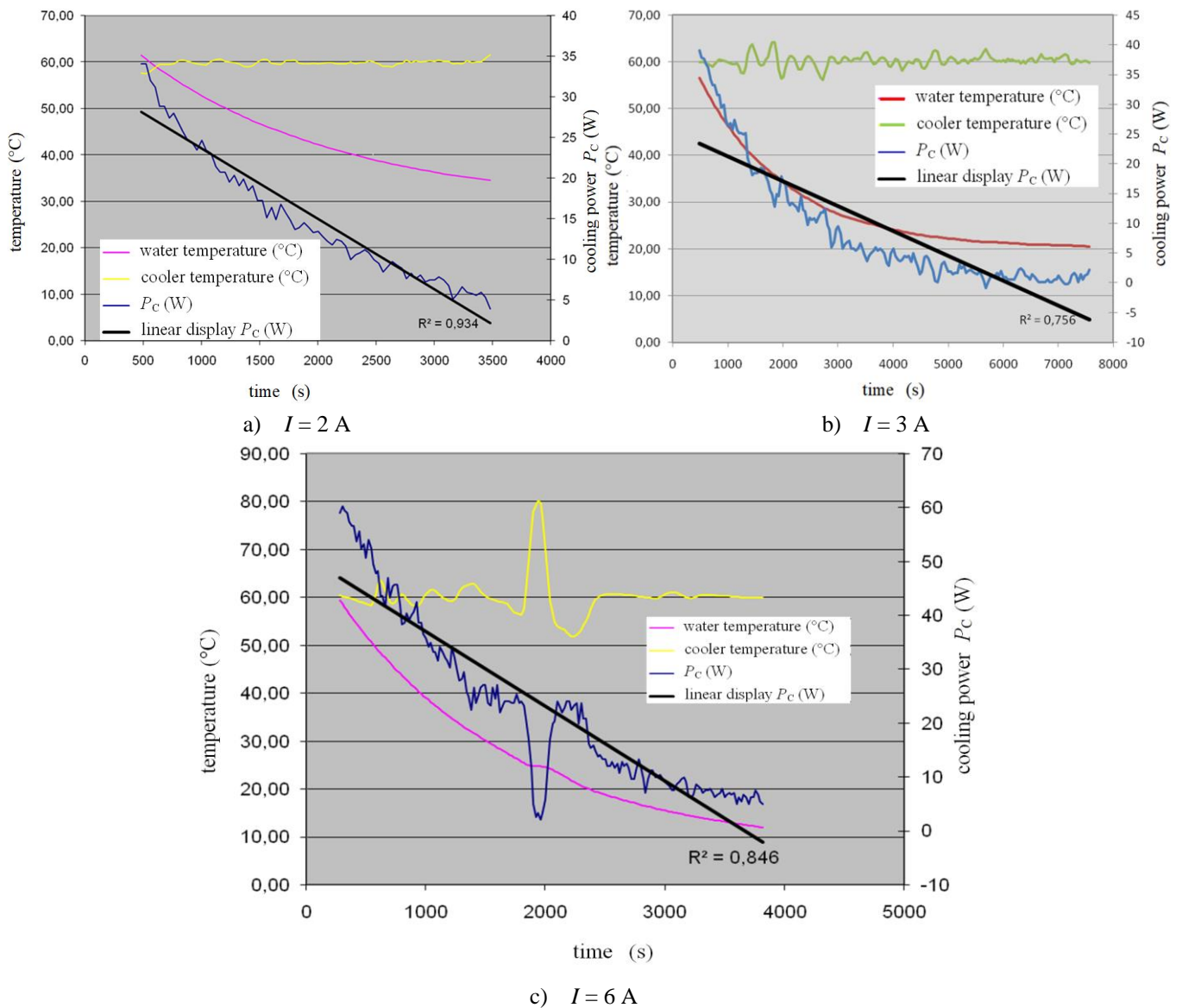


**FIGURE 8: Graphical dependence of individual characteristics at different current loads**

The goal of the measurements was to achieve the largest possible temperature difference between the temperature of the cooler (the temperature of the warm side of the Peltier cell) and the temperature of the cooled water in the cylinder. The temperature difference is a direct indicator of the cooling of the water by the Peltier cell (fig. 9).

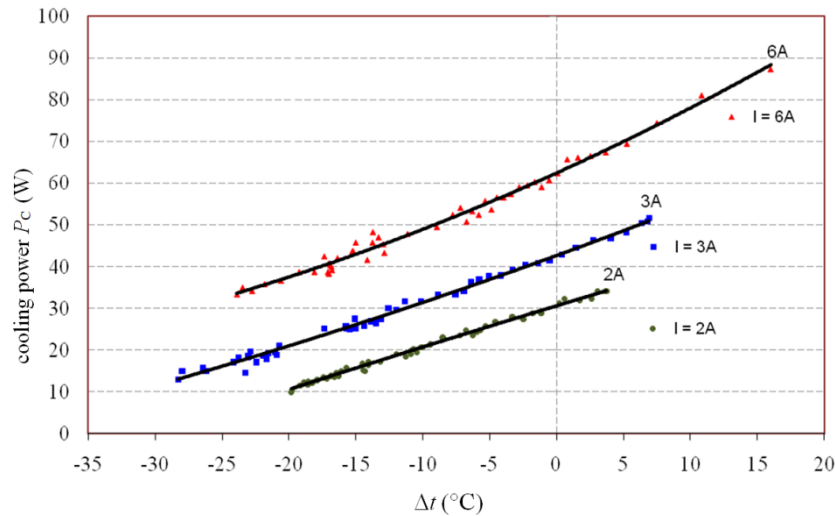


**FIGURE 9: Comparison of PC cooling performance at different current loads**

As the temperature of the water in the cylinder changes, so does the cooling capacity. The warmer the water in the cylinder, the more cooling power is needed to cool it. The colder the water in the cylinder, the less power the Peltier cell operates.

#### IV. CONCLUSION

The heated water itself simulates the temperature of the processor working in the given conditions. In fact, the more the processor is loaded, the more it heats up, which means it produces more heat into the computer environment, which must be perfectly dissipated. Imperfect removal of heat from the surface of the processor leads to a decrease in performance, frequency speed and, in case of long-lasting high temperature, to its destruction and deterioration. Therefore, the combination of cooling, which was discussed in the article, is the suitable alternative to the possible cooling used in the process of cooling semiconductor components with a Peltier cell. With its properties, the Peltier cell absorbs the heat of the heated water in the steel cylinder (or the processor), thereby cooling it (or the processor). The heat generated on the other side of the Peltier cell is removed by the cooler, i.e. heat is transferred between the warm side of the Peltier cell and the cold surface of the cooler. The heat dissipation is enhanced by the used fan for perfect heat dissipation from the cooler and into the surroundings. This method of combining cooling with subsequent heat removal makes it possible to use the processor at higher frequency speeds.

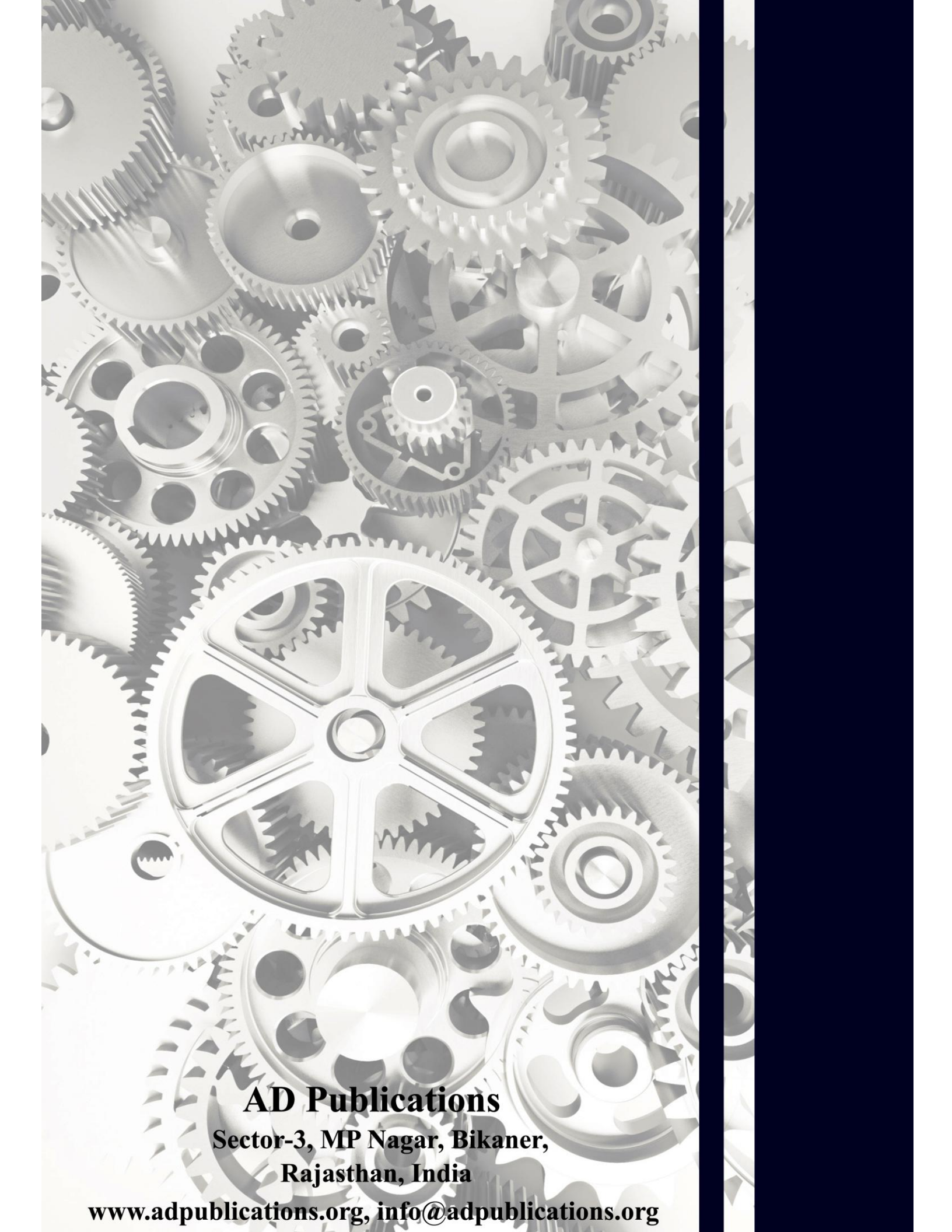
Cooling with Peltier cells represents a progressive way of implementing a cooling system. It is a suitable alternative wherever it is necessary to extract a large heat flow from a small area or where emphasis is placed on the small dimensions of the cooling system. Peltier cells also play an important role in temperature regulation.

#### ACKNOWLEDGEMENTS

This paper was written with the financial support from the VEGA granting agency within the Projects No. 1/0224/23 and No. 1/0532/22, from the KEGA granting agency within the Project No. 012TUKÉ-4/2022, and with the financial support from the APVV granting agency within the Projects No. APVV-15-0202, APVV-20-0205 and APVV-21-0274.

#### REFERENCES

- [1] Remeli, MF, et al.: *Experimental study of a mini cooler by using Peltier thermoelectric cell*. IOP Conference Series: Materials Science and Engineering, 788 (2020), 012076.
- [2] Sajid, M., Hassan I., Rahman A.: *An overview of cooling of thermoelectric devices*. Renew. Sustain. Energy Rev. 78 (2017), p.15-22.
- [3] Cao, L., Han, J., Duan L., Huo C.: *Design and Experiment Study of a New Thermoelectric Cooling Helmet*. Procedia Eng. 205 (2017), p.1426-1432.
- [4] Rohsenow, Warren M., et al.: *Handbook of Heat Transfer*, McGraw-Hill, 3. edition, (1998), ISBN 978-0-07-053555-8
- [5] Casano, G., Piva, S.: *Experimental investigation of a Peltier cells cooling system for a Switch-Mode Power Suppl*. Microelectronics Reliability 79 (2017), p.426-423.



**AD Publications**

**Sector-3, MP Nagar, Bikaner,  
Rajasthan, India**

**[www.adpublications.org](http://www.adpublications.org), [info@adpublications.org](mailto:info@adpublications.org)**